In Vitro Cell Line Studies

7.1 CELL AND CULTURE CONDITIONS

B16F10, a highly metastatic lung selected subline derived from C57BL/6 murine melanoma was purchased from National Centre for Cell Science, Pune, India. The cell line was maintained as a continuous culture in IMDM (Iscove's Minimum Dulbecco's medium), supplemented with 10 % fetal bovine serum (FBS), 100 U/ml penicillin and 100 µg/ml streptomycin. Cells were grown in a humidified atmosphere of 5 % CO_2 and 95 % air and media was replenished every third day.

7.2 MATERIALS

Plastic wares were purchased from Tarson India Ltd, Mumbai. Fetal bovine serum (FBS) was purchased from Biowest, Genetix, India. Iscove's Minimum Dulbecco's Medium (IMDM), MTT A.R. (3-(4, 5-dimethyl-2-yl)-2,5-diphenyl tetrazolium bromide) and RNAse were procured from Himedia Lab. Pvt. Ltd., Mumbai, India. Propidium iodide was purchased from Sigma Aldrich, Mumbai, India. Sodium chloride (NaCl), potassium chloride, disodium hydrogen phosphate, potassium dihydrogen phosphate and sodium EDTA were purchased from S.D. Fine-chem Ltd, Mumbai. Required dye like eosin, hematoxilin, crystal violate of analytical grade were provided by ACTREC, Navi Mumbai and used without further purification.

7.3 METHODS

7.3.1 Cytotoxicity assay

Cytotoxicity assay were performed as reported earlier (Dua & Gude, 2006; Liu et al., 2008). Briefly, B16F10 cells were harvested in exponential phase and seeded in 96 well flat bottom tissue culture plate at a concentration of 4 X 10^3 cells/100 µl/well. The cells were allowed to grow and stabilize for 24 h in incubator at 37 °C with 5 % CO_2. Subsequently, the cells were treated with serial concentrations of plain ETO and micellar formulations prepared in complete medium and incubated for 24 h. Plain ETO used for study, was dissolved in DMSO and final concentration of DMSO was kept at 0.1 %. Each treatment was performed in six well replicates. Post treatment cells were washed with PBS and to this 20 µl of MTT in PBS (5 mg/ml) and 80 µl of complete media were added to each well and incubated for 4 h at 37 °C. Plates were then centrifuged at 1500 rpm for 20 min. Medium was aspirated from the wells and 100 µl of DMSO was added to each well and kept on shaker for 10 min to dissolve formazan crystals. The optical density was measured in an enzyme linked

immuno sorbant assay (ELISA) plate reader (Molecular Devices, Spectra Max 190 with Softmax Pro) at 540 nm with a reference wavelength of 690 nm.

For 48 and 72 h drug incubation study, B16F10 cells were seeded at concentration of 2 X 10^3 cells/100 µl/well & 1.5 X 10^3 cells/100 µl/well respectively and cells were incubated in presence of drug for respective time point. Percent cell viability was plotted against concentration and IC_{50} values were determined from the dose effect curve at the drug concentration that decreased the cell viability to 50 %. Results were expressed as mean ± S.D. and were representatives of three independent experiments.

7.3.2 Cytopathic study

Cytopathic assay was performed to see the effect of plain ETO and micellar formulations on cell morphology (Dua & Gude, 2006). Briefly, 2 X 10^4 B16F10 cells/ml were seeded in 40 mm tissue culture plates containing heat sterilized coverslips and incubated at 37 °C for 48 h.. Afterward, cells were treated with half and quarter IC_{50} dose of ETO and micellar formulations in complete medium for 48 h and washed with PBS. Cells were fixed with cold methanol and stained with haemotoxilin and eosin (Lillie, 1965). In final step, cover slips were washed with alcohol to remove excess dye, mounted and fixed on the slide with DPX solution. Cells were examined under a Zeiss AxioImager Z-1 microscope (Germany) and images were taken.

7.3.3 Colony forming assay

Colony formation assay was carried out as described previously with minor changes (Franken et al., 2006). Briefly, 40 mm tissue culture plate was seeded with 600 cells of B16F10 in complete medium and allowed to grow for 24 h. The cells were incubated with ETO and micellar formulations at half and quarter IC_{50} dose for 48 h. Cells were washed with PBS and incubated further for 48 h in complete medium to grow colony well. Each treatment was done in triplicate. The colonies obtained were washed with PBS and fixed with cold methanol for 2 min followed by staining with 0.5 % crystal violet. Colonies with 50 or more number of cells were counted on a Zeiss inverted light microscope (Germany) with the help of Palm Robo Software and percent colony inhibition was calculated using following formula.

$$\% \text{ colony inhibition} = 100 - \frac{\text{Number of colonies in Formulation}}{\text{Number of colonies in UC}} \times 100$$

7.3.4 Cell migration assay

Cell migration assay were performed to estimate the migration rate of B16F10 cells after drug treatment (Dua & Gude, 2008). B16F10 cells at density of 2 X 10^4 cells/ml in complete medium were added to 40 mm tissue culture plates and incubated for 48 h. The monolayer was treated with ETO and micellar formulations at sub toxic concentration ($IC_{12.5}$ and IC_{25}) and kept for 48 h incubation at 37 °C with 5 % CO_2. After treatment, cells were washed with PBS and wound was created in triplicate using sterile tip. The pealed off cells were removed with two PBS washes and cells were incubated further for 48 h in IMDM with 0.1 % FBS for wound coverage. Cells were washed with PBS, fixed with cold methanol and stained with 0.5 % crystal violet. A zero h reference plate was fixed immediately after wound creation.

Migration of cell from the edge of the injured monolayer was measured using Laser Capture Microdissection Microscope [LCMM, Zeiss, Germany] along with Palm Robo software at 25 different positions. With reference to zero h plate, percent relative wound width and percent cell migration were calculated using formula given below

$$\% \text{ relative wound width} = \frac{\text{Wound width of UC or formulation}}{\text{Wound width at zero h}} \times 100$$

$$\% \text{ cell migration} = \frac{\text{Zero h wound width} - \text{treated wound width}}{\text{Zero h wound width} - \text{untreated wound width}} \times 100$$

7.3.5 Cell adhesion study

Cell adhesion study were carried out to find out the adhesion ability of B16F10 cells after treatment with ETO and micellar formulations as well as to check the inherent adhesive properties of ligand after conjugations to micelles (Lopez et al., 2004; Dua et al., 2007). The study was performed with slight modification as reported by Yamamura et al. (1993) using peptides as substrates instead of laminin and fibronectin as substrate. Briefly, flat bottom 96 well plates were coated with 50 µl of peptides YIGSR-NH_2/EILDV-NH_2 (0.2 mg/ml in PBS) and plates were incubated

overnight at 37 °C for polymerization. Unpolymerized substrates were washed with PBS and the plates were blocked with 1 % BSA in PBS for 2 h at 37 °C.

Sub confluent B16F10 cells were treated with half IC_{50} concentration of ETO and micellar formulations for 48 h. The cells were harvested using saline EDTA, washed and diluted to a final concentration of 3 X 10^5 cells/ml in IMDM containing 0.1 % BSA. A 100 µl of cell suspension was added to each substrate coated well and incubated at 37 °C for 1 h. Non adherent cells were removed washing twice with PBS and to plates 100 µl of IMDM and 20 µl of MTT (5 mg/ml) were added and kept for 4 h incubation and centrifuged at 1500 rpm for 20 min. Supernatant was removed and 100 µl of DMSO/well added and readings were measured using ELISA plate reader (Molecular Devices, Spectra Max 190 with Softmax Pro) at 540 nm with reference wavelength of 690 nm. Wells containing unwashed cells were kept as control. The adherent cells were quantified using MTT assay and expressed as relative % of the respective total unwashed cells.

7.3.6 Confocal microscopy

Uptake of 6-coumarin loaded micellar formulations by B16F10 cells were visualized by confocal laser scanning microscope (Yuancai et al., 2007). Briefly, B16F10 cells at density of 2 X 10^4 cells/ml were seeded in 40 mm tissue culture plates containing heat sterilized coverslips. When cells reached to 70 % confluency, was treated with 6-coumarin loaded micellar formulations (300 µg/ml) in complete media for 1 h or 3 h. Cells were washed with PBS twice and fixed with 4 % paraformaldehyde in PBS for 15 min at 37 °C. Coverslips were mounted using 4 % DABCO (fluorescent mounting medium) and confocal images were taken using FITC filter (Ex (l) 495 nm, Em (l) 520 nm) by Confocal Laser Scanning Microscope (Zeiss LSM S10 Meta, Germany).

7.3.7 Cell uptake study

Cell uptake studies were carried out to determine the intracellular uptake of ETO by B16F10 cells after incubation period of 2 h. In addition to plain ETO, MPCL235 and MPCL570 micellar formulations, peptide YIGSR-NH_2 and EILDV-NH_2 conjugated micelles prepared with different surface density of peptide (YIGSR-NH_2/ EILDV-NH_2) i.e. 5 %, 10 % and 20 % were also evaluated for their maximum receptor mediated cellular uptake (Zhao & Yung, 2008). The cellular content of ETO was

determined by developed HPLC method using diazepam as internal standard (Chapter 3.1.2). Briefly, 4 X 10^4 B16F10 cells/ml were added to 90 mm tissue culture plates and allowed to grow to 90 % confluency. Cells were treated with plain ETO or micellar formulations at drug concentration of 20 µg/ml for 2 h at 37 °C. Cells were washed with ice cold PBS twice and harvested with saline EDTA. The final count of cell was made to 2 X 10^6 cells/ml and centrifuged at 1000 rpm for 15 min. After resuspending cell in PBS, cells were lysed by probe sonicator (Branson Sonifier S-450, USA) for 3 min at 60 % duty cycle and further procedure was followed as mentioned in chapter 3.1.2.3.

The protein content in the cell lysate was measured by Bradford's method using bovine serum albumin as standard. The percentage uptake of drug were calculated using following formula as reported earlier (Yuan et al., 2008)

$$\text{Drug uptake percentage (\%)} = \frac{C/M}{Ci/Mi} \times 100$$

where C is the intracellular concentration of ETO measured by HPLC, M the unit weight (milligram) of cellular protein after incubation, Ci the initial concentration of ETO, and Mi is the initial unit weight (milligram) of cellular protein.

7.3.8 Cell cycle analysis by flow cytometry

B16F10 cells at density of 2 X 10^4 cells/ml were seeded to 60 mm tissue culture plates and incubated for 24 h (Dua & Gude, 2006). Cells were treated with quarter and half IC_{50} concentration of ETO and micellar formulations and incubated for 48 h. After harvesting, the final count of cells was made to 1 X 10^6 cells/ml. Cells were washed with PBS twice, fixed with chilled 70 % alcohol. The cell suspension was spin down at 1000 rpm for 10 min, washed with PBS and pellets were resuspended in 350 µl of PBS. RNA was removed by adding 10 µl of RNAse (10 mg/ml) and kept at 37 °C for 15 min and to this 50 µl of propidium iodide (1 mg/ml) was added. Tubes were kept in dark in ice until use. Ten thousand events were acquired on Becton-Dickinson FACS SCAN and analyzed using Modfit software.

7.4 RESULTS AND DISCUSSION

7.4.1 Cytotoxicity assay

The *in vitro* cytotoxic activity of plain ETO and ETO loaded micellar formulation on B16F10 cells were expressed as % cell viability with various drug incubation time i.e. 24, 48 and 72 h as represented in Table 7.1 to 7.7. The IC_{50} values for plain ETO and ETO loaded micellar formulation were derived from cytotoxicity profile obtained and are shown in Table 7.8.

The micellar formulations exhibited *in vitro* anticancer activity comparable to that of free ETO (Fig. 7.1 to Fig. 7.6 and Table 7.8). Both ETO and ETO loaded micellar formulations displayed resembling concentration and time dependent cytotoxicity. Plain ETO at 24, 48 and 72 h incubation time exhibited IC_{50} values of 0.087, 0.050 and 0.043 μM respectively. After 24 h incubation period, the calculated IC_{50} values of micellar formulations were upto 25 to 50 times higher compared to plain ETO (Table 7.8). Based on these findings, it was observed that micelles with lower molecular weight (5500) showed higher cytotoxicity compared to micelles with higher molecular weight (12000). Reasonable explanation could be deduced from the core shell structure of micelles which having different release profile of drug observed during *in vitro* release studies conducted. The sustained release of the drug loaded micelles determines that certain time is required to release the drug into the culture medium or inside cell after endocytosis. When incubated with the cells, the drug concentration of ETO loaded micelles slowly increased due to its sustained release profile. Plain ETO showed higher cytotoxic effect at 24 h incubation time compared to micellar formulation, since it is in soluble form and can diffuse in to cells quickly. Earlier findings with plain drug doxorubicin and cisplatin also showed similar cytotoxicity profile compared to nanoparticulate system at initial incubation time points (Zhao & Yung, 2008; Li et al., 2008)

Concentration (μM)	Plain ETO		
	% Viability of B16F10 cells at various incubation time period		
	24 h	48 h	72 h
0	100.00 ± 7.27	100.00 ± 2.71	100.00 ± 2.90
0.025	93.38 ± 5.84	59.57 ± 5.40	58.03 ± 4.84
0.050	85.12 ± 3.88	49.46 ± 7.40	46.55 ± 3.94
0.10	70.85 ± 7.52	42.55 ± 4.57	30.01 ± 5.27
0.50	58.80 ± 8.55	39.36 ± 3.59	13.93 ± 5.16
1.0	47.93 ± 8.62	29.25 ± 2.50	10.71 ± 4.86
10.0	23.14 ± 6.42	12.76 ± 2.59	6.58 ± 3.48
50.0	12.39 ± 7.66	9.04 ± 1.32	3.36 ± 2.27
IC_{50}	**0.087**	**0.050**	**0.043**

Table 7.1 Percent viability of B16F10 cells treated with various concentrations of ETO at different incubation time period (Results are mean ± S.D. of three individual experiments)

Concentration (μM)	MPCL235		
	% Viability of B16F10 cells at various incubation time period		
	24 h	48 h	72 h
0	100.00 ± 7.27	100.00 ± 2.71	100.00 ± 2.9
0.025	83.71 ± 9.67	79.25 ± 4.79	59.87 ± 3.32
0.050	78.85 ± 6.23	56.38 ± 5.85	37.67 ± 6.50
0.10	75.71 ± 4.10	47.93 ± 4.85	22.53 ± 4.36
0.50	66.14 ± 9.52	32.44 ± 3.19	12.71 ± 3.85
1.0	55.85 ± 7.12	26.06 ± 4.30	10.41± 6.17
10.0	40.28 ± 6.66	13.29 ± 2.12	6.89 ± 2.44
50.0	32.57 ± 5.20	7.44 ± 3.03	4.59 ± 3.33
IC_{50}	**4.3**	**0.082**	**0.034**

Table 7.2 Percent viability of B16F10 cells treated with various concentrations of MPCL235 at different incubation time period (Results are mean ± S.D. of three individual experiments)

Concentration (μM)	YPCL235		
	% Viability of B16F10 cells at various incubation time period		
	24 h	48 h	72 h
0	100.00 ± 5.14	100.00 ± 4.32	100.00 ± 7.13
0.025	80.40 ± 4.76	68.15 ± 3.52	23.31 ± 4.17
0.050	74.03 ± 8.64	45.50 ± 4.23	13.71 ± 3.50
0.10	66.17 ± 7.93	39.79 ± 4.53	10.42 ± 5.44
0.50	58.21 ± 7.32	30.15 ± 7.40	8.64 ± 3.17
1.0	52.63 ± 9.22	17.46 ± 5.29	9.19 ± 5.07
10.0	30.08 ± 10.55	13.22 ± 3.05	6.31 ± 3.26
50.0	20.32 ± 8.34	6.84 ± 2.79	3.29 ± 2.2
IC_{50}	**2.2**	**0.040**	**0.014**

Table 7.3 Percent viability of B16F10 cells treated with various concentrations of YPCL235 at different incubation time period (Results are mean ± S.D. of three individual experiments)

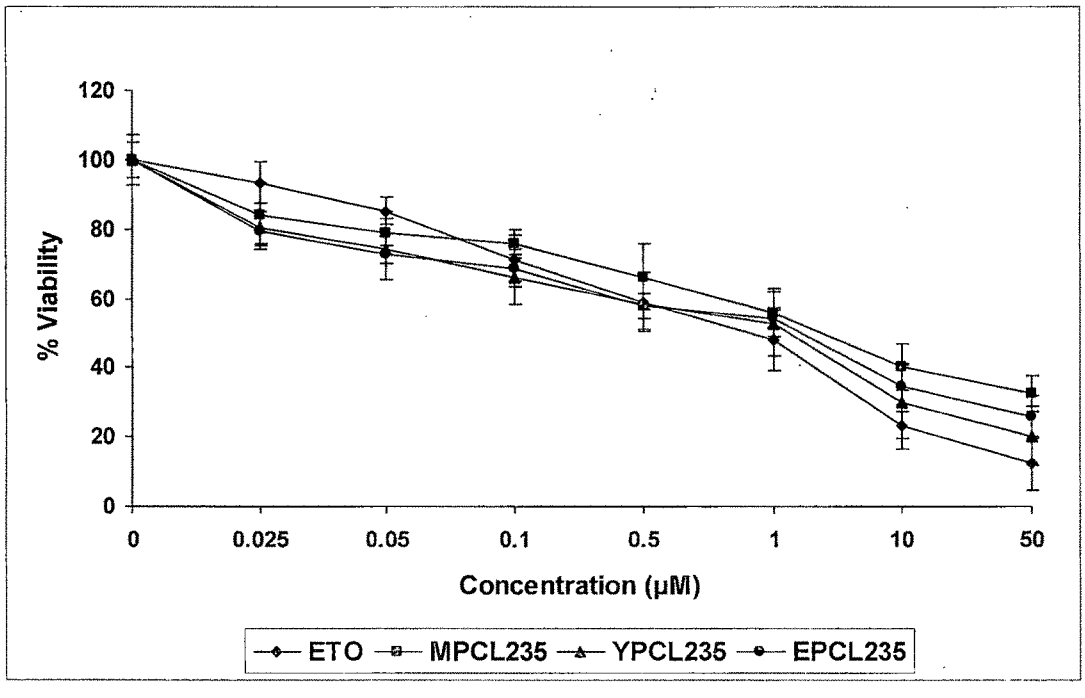

Figure 7.1 Cell viability of B16F10 cells with ETO, MPCL235, YPCL235 and EPCL235 formulation after 24 h incubation period

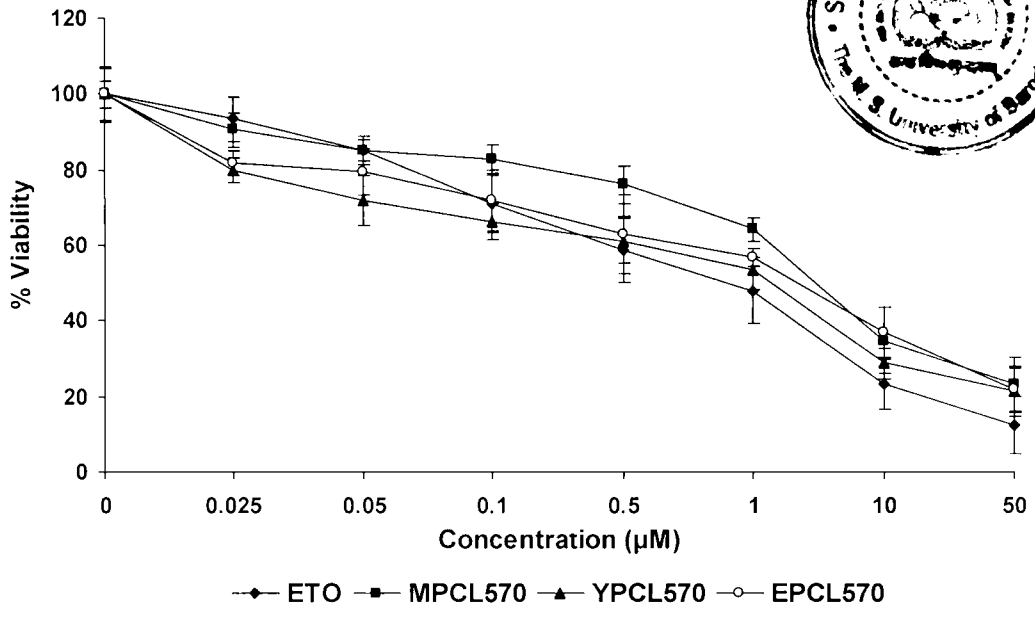

Figure 7.2 Cell viability of B16F10 cells with ETO, MPCL570, YPCL570 and EPCL570 formulation after 24 h incubation period

Extending the incubation time to 48 h, led to noticeable lowered cell viability at each dose compared to that of 24 h for plain ETO and micellar formulations. The calculated IC_{50} values for MPCL235, YPCL235 and EPCL235 were 0.082, 0.040 & 0.055 µM respectively (Table 7.8). At the same time, MPCL570, YPCL570 and EPCL570, the IC_{50} values obtained were 0.120, 0.045 & 0.075 µM respectively. MPCL235 and MPCL570 showed 1.6 and 2.4 fold lower cytotoxicity respectively compared to plain ETO at 48 h incubation (Table 7.8). Peptide conjugated micelles YPCL235, EPCL235, YPCL570 and EPCL570 showed higher cytotoxicity compared to non-conjugated micelles but the effect was still comparable to plain ETO. After 72 h incubation period, plain ETO showed no further significant increase in cytotoxicity compared to 48 h, while a major reduction in cell viability were observed with all micellar formulations. The calculated IC_{50} values of all micellar formulations were lower than plain ETO. MPCL235 and MPCL570 showed a little increase in cytotoxic effect compared to plain ETO as shown in Table 7.8. Peptide YIGSR-NH_2 conjugated micelles YPCL235 and YPCL570 showed 3.0 fold and 2.1 fold increases in toxicity respectively compared to plain ETO. EILDV-NH_2 conjugated micelles EPCL235 and EPCL570 showed increase in cytotoxic effect of 1.7 and 1.4 fold compared to plain ETO.

Concentration (μM)	EPCL235		
	% Viability of B16F10 cells at various incubation time period		
	24 h	48 h	72 h
0	100.00 ± 5.14	100.00 ± 4.32	100.00 ± 7.13
0.025	79.42 ± 4.31	71.42 ± 3.90	50.61 ± 3.25
0.050	72.57 ± 2.71	51.13 ± 2.25	30.86 ± 2.17
0.10	68.57 ± 3.81	45.76 ± 2.11	11.93 ± 4.57
0.50	57.71 ± 3.48	36.74 ± 2.11	9.46 ± 3.72
1.0	54.28 ± 2.94	23.86 ± 3.70	8.09 ± 3.52
10.0	34.28 ± 6.83	18.51 ± 2.64	5.21 ± 2.30
50.0	25.71 ± 6.33	7.4 ± 2.79	3.29 ± 3.10
IC_{50}	**2.5**	**0.055**	**0.025**

Table 7.4 Percent viability of B16F10 cells treated with various concentrations of EPCL235 at different incubation time period (Results are mean ± S.D. of three individual experiments)

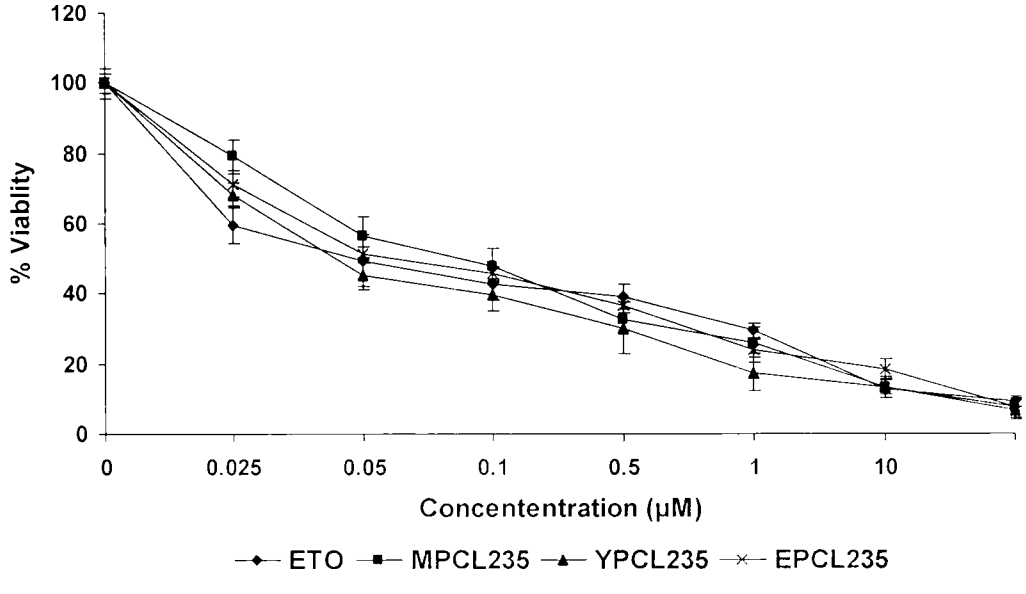

Figure 7.3 Cell viability of B16F10 cells with ETO, MPCL235, YPCL235 and EPCL235 formulation after 48 h incubation period

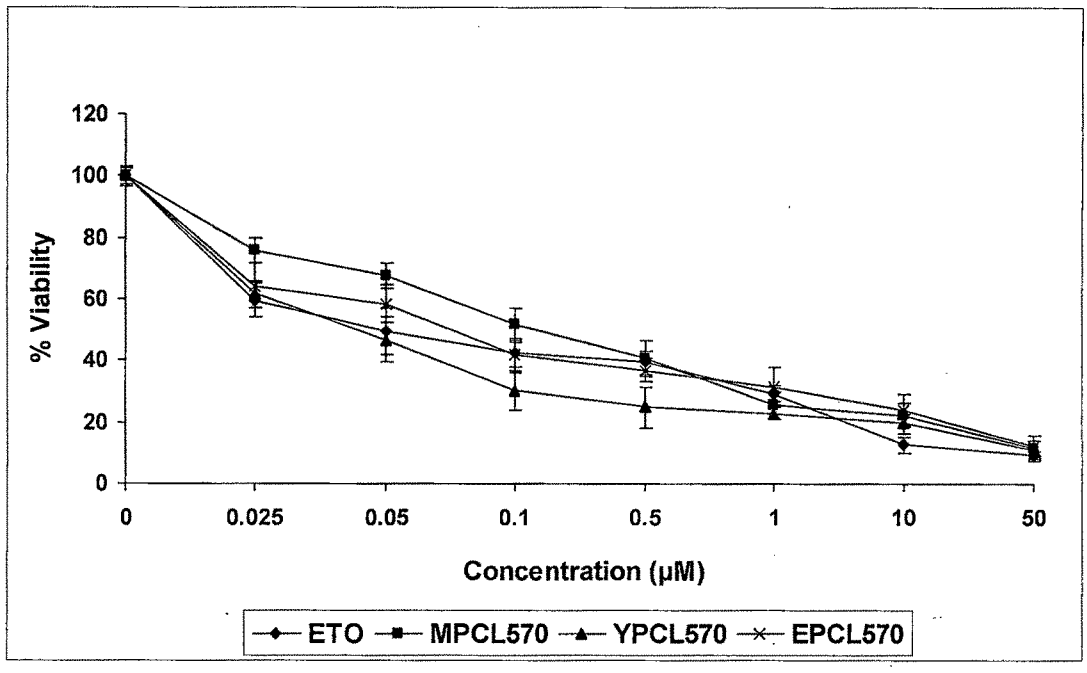

Figure 7.4 Cell viability of B16F10 cells with ETO, MPCL570, YPCL570 and EPCL570 formulation after 48 h incubation period

Concentration (µM)	MPCL570		
	% Viability of B16F10 cells at different time incubation		
	24 h	48 h	72 h
0	100.00 ± 3.43	100.00 ± 2.94	100.00 ± 4.8
0.025	90.58 ± 4.45	75.79 ± 4.15	62.20 ± 5.13
0.050	85.00 ± 2.95	67.53 ± 4.29	43.26 ± 6.2
0.10	82.64 ± 3.91	51.59 ± 5.49	19.20 ± 4.76
0.50	75.88 ± 5.03	40.76 ± 5.84	10.53 ± 3.63
1.00	64.11 ± 3.02	25.47 ± 4.23	8.66 ± 4.61
10.0	34.70 ± 8.55	22.29 ± 3.9	4.13 ± 2.34
50.0	22.94 ± 7.38	11.46 ± 2.71	2.40 ± 4.11
IC_{50}	**5.0**	**0.120**	**0.040**

Table 7.5 Percent viability of B16F10 cells treated with various concentrations of MPCL570 at different incubation time period (Results are mean ± S.D. of three individual experiments)

Concentration (μM)	YPCL570		
	% Viability of B16F10 cells at different time incubation		
	24 h	48 h	72 h
0	100.00 ± 3.43	100.00 ± 2.94	100.00 ± 4.51
0.025	80.00 ± 3.30	61.68 ± 4.41	44.00 ± 3.91
0.050	71.76 ± 6.55	46.75 ± 7.14	17.46 ± 3.41
0.10	66.17 ± 4.88	30.06 ± 5.97	12.80 ± 4.78
0.50	61.11 ± 6.01	24.83 ± 6.53	11.60 ± 2.57
1.00	53.52 ± 5.54	22.87 ± 2.07	9.33 ± 3.22
10.0	28.63 ± 4.16	19.56 ± 3.10	5.06 ± 2.94
50.0	21.17 ± 6.66	11.08 ± 2.68	2.80 ± 2.31
IC_{50}	**2.8**	**0.045**	**0.020**

Table 7.6 Percent viability of B16F10 cells treated with various concentrations of YPCL570 at different incubation time period (Results are mean ± S.D. of three individual experiments)

Concentration (μM)	EPCL570		
	% Viability of B16F10 cells at different time incubation		
	24 h	48 h	72 h
0	100.00 ± 6.86	100.00 ± 3.20	100.00 ± 4.51
0.025	81.76 ± 3.13	64.17 ± 7.29	62.32 ± 3.91
0.050	79.20 ± 6.11	58.28 ± 6.13	27.20 ± 3.41
0.10	71.79 ± 7.93	41.66 ± 4.83	14.88 ± 4.78
0.50	62.67 ± 10.45	36.89 ± 3.64	11.74 ± 2.57
1.00	56.82 ± 2.38	31.55 ± 6.14	10.46 ± 3.22
10.0	36.88 ±6.42	24.06 ± 4.81	5.93 ± 2.94
50.0	21.65 ± 5.73	12.29 ± 3.26	3.72 ± 2.31
IC_{50}	**3.1**	**0.075**	**0.031**

Table 7.7 Percent viability of B16F10 cells treated with various concentrations of EPCL570 at different incubation time period (Results are mean ± S.D. of three individual experiments)

Formulation	IC50 at different time point incubation (μM)		
	24 h	48 h	72 h
ETO	0.087	0.050	0.043
MPCL235	4.3	0.082	0.034
YPCL235	2.2	0.040	0.014
EPCL235	2.5	0.055	0.025
MPCL570	5.0	0.120	0.040
YPCL570	2.8	0.045	0.020
EPCL570	3.1	0.075	0.031

Table 7.8 Inhibitory concentration (50 %) of various formulations at different time incubation with B16F10 cells

The peptide conjugated and non-conjugated micelles loaded with ETO exhibited higher anticancer activity against B16F10 cells to that of plain ETO as time proceeds. The results obtained indicates that ETO after entrapment in the micelles will provide more selective delivery of ETO to tumors in vivo due to the EPR effect as well by receptor mediated uptake. There are two possible mechanism by which the micellar systems exhibits it cytotoxic effect, one in which the drug releases extracellular and than reach to cell by simple diffusion or by endocytosis process in which the carrier will release drug intracellularly. Moreover, a P-gp efflux which is commonly observed with free drugs in case of multidrug resistant cell, which is not seen in polymer-drug conjugates or drug encapsulated polymeric micelles, which most likely transported to cell via endocytosis route (Xiaoqiang et al., 2008). It was reported that MPEG-PCL micelles plays a MDR modulator with prevention of P-gp mediated reflux. (Xiaoqiang et al., 2008; Zastre et al., 2008).

The cytotoxicity of ETO loaded micelles conjugated with peptides against B16F10 cells was much greater than that of ETO loaded non conjugated micelles because of higher cellular uptake. The similar findings were reported by many authors, suggesting internalization of micellar carrier by receptor mediated mechanism and hence higher amount of drug available inside cells (You & Park, 2004; Zhao & Yung, 2008; Xiaoqiang et al., 2008). They reported that the folate conjugated nanocarrier loaded with drug have higher toxicity and cellular uptake because of folate receptor

overexpressed on cells. However, immunochemistry studies have shown the over-expression of folate receptors in normal tissues like placenta and kidney, which raises some issues for possible clinical translation of folate bioconjugates (Alexis et al., 2008). Peptide conjugated liposomes and micelles loaded with anticancer drug showed the higher uptake of nanocarrier (Lopez et al., 2004; Nasongkla et al., 2004) with use of cell adhesion peptide YIGSR & cyclic RGD. They reported that peptide conjugated systems have higher cytotoxicity compared to non conjugated one supporting the receptor mediated mechanism of targeting.

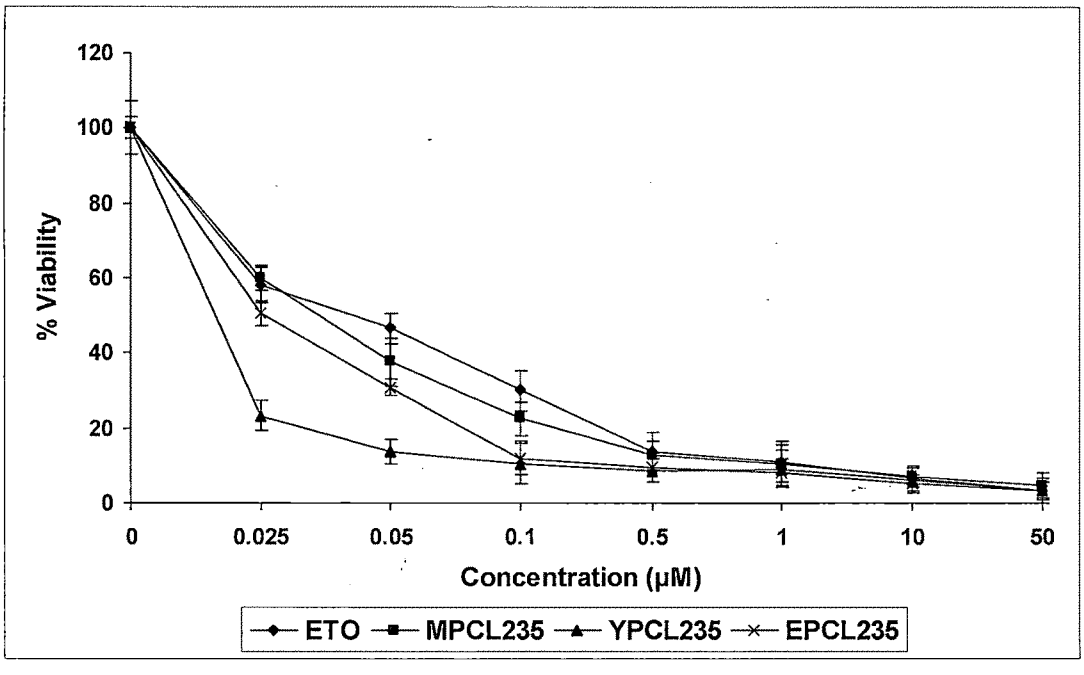

Figure 7.5 Cell viability of B16F10 cells with ETO, MPCL235, YPCL235 and EPCL235 formulation after 72 h incubation period

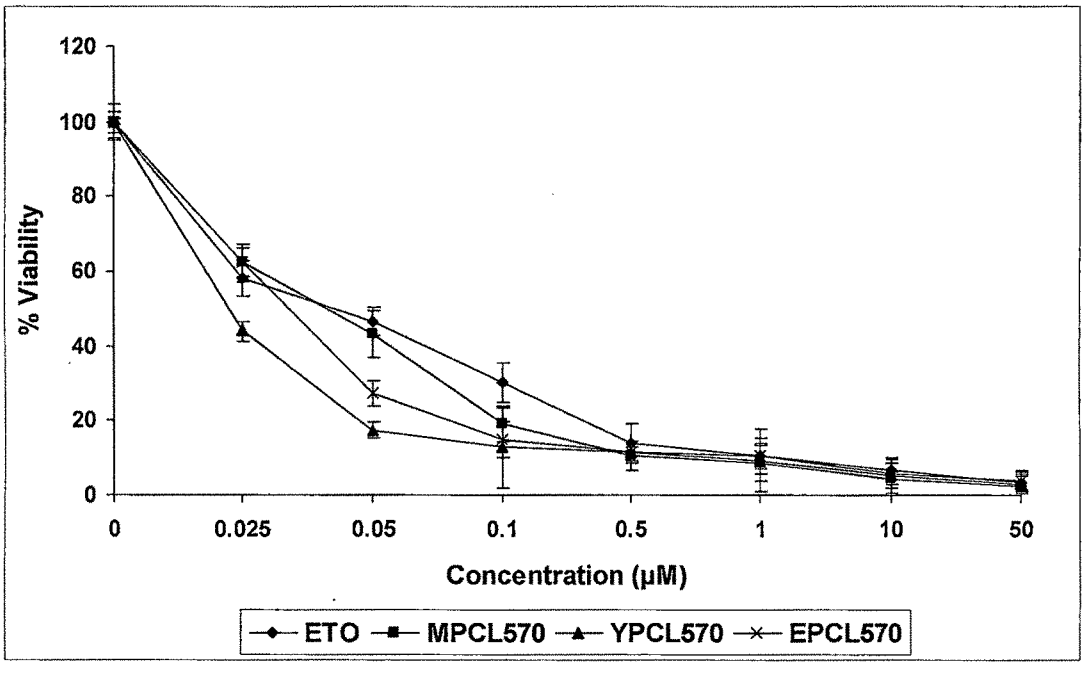

Figure 7.6 Cell viability of B16F10 cells with ETO, MPCL570, YPCL570 and EPCL570 formulation after 72 h incubation period

It is required that the nanocarrier used should be safe and nontoxic. The micellar formulations were consisted of two polymers PEG and PCL which are US FDA approved for drug delivery system. However, it is required to know the effect of the method of synthesis of polymer and formulation on cytotoxicity of cells. Placebo micellar formulations MPCL235-P and MPCL570-P were tested at similar polymer concentration of MPCL235 and MPCL570 used in study and the cytotoxic effects were evaluated at three different time incubation period (Table 7.9). At maximum concentration of polymer 800 μg/ml, both MPCL235-P and MPCL570-P did not show any cytotoxic effect, implies that polymer used as a carrier for ETO is safe to use (Figure 7.7 & 7.8).

Formulation	% Viability of B16F10 cells at different time of incubation			
	Concentration of polymer (µg/ml)	24 h	48 h	72 h
MPCL235-P	0	100.00 ± 6.86	100.00 ± 5.65	100.00 ± 3.51
	16	97.47 ± 8.39	98.06 ± 6.20	101.5 ± 6.71
	160	95.11 ± 7.09	94.65 ± 4.28	95.23 ± 4.15
	800	96.07 ± 5.13	96.17 ± 2.13	96.48 ± 3.95
MPCL570-P	0	100.00 ± 4.73	100.00 ± 3.20	100.00 ± 5.02
	16	98.88 ± 3.31	103.10 ± 6.41	96.16 ± 4.35
	160	93.47 ± 5.46	108.02 ± 7.11	99.41 ± 3.74
	800	92.87 ± 7.56	96.79 ± 6.86	98.34 ± 6.04

Table 7.9 Percent viability of B16F10 cells treated with various concentrations of MPCL235-P and MPCL570-P at different incubation time period (Results are mean ± S.D. of three individual experiments)

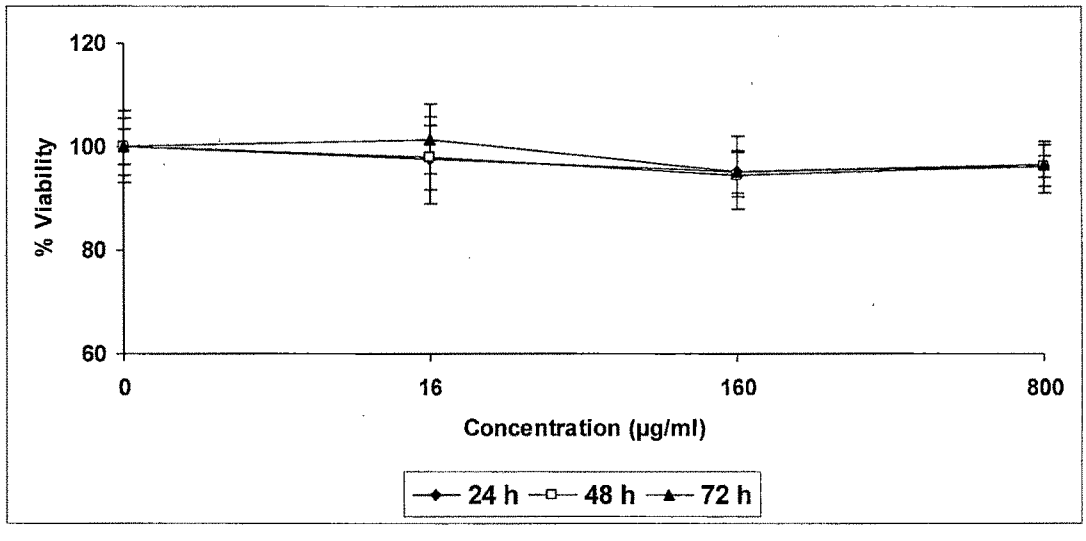

Figure 7.7 Cell viability of B16F10 cells after treatment with MPCL235-P for various time point incubation

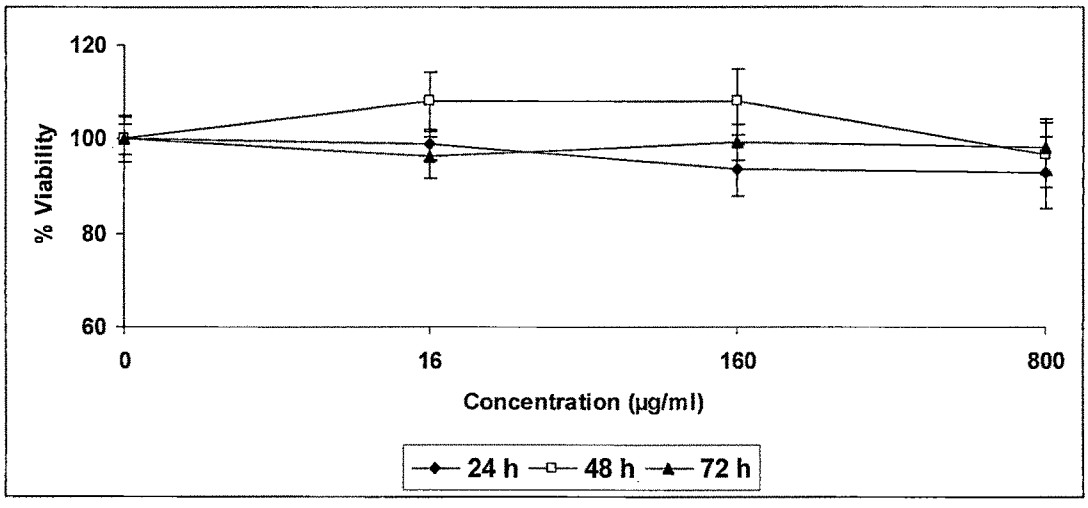

Figure 7.8 Cell viability of B16F10 cells after treatment with MPCL570-P for various time point incubation

Based on the finding obtained from cytotoxicity studies, further *in vitro* cell line studies were carried out at subtoxic concentration of plain ETO and ETO loaded micellar formulation. The studies were carried out at half and quarter dose of IC_{50} value i.e. at IC_{25} and $IC_{12.5}$ dose, derived after 48 h incubation. Table 7.10 represents the subtoxic concentration dose and formulation code denoted for respected formulation in rest of *in vitro* cell line studies.

Formulations	Formulation code (subtoxic dose)*	Dose of ETO (μM) (Half and quarter IC_{50} dose, 48 h incubation)
Plain ETO	ETO- A	0.025
	ETO- B	0.012
MPCL235	MPCL235-A	0.041
	MPCL235 –B	0.020
YPCL235	YPCL235- A	0.020
	YPCL235- B	0.010
EPCL235	EPCL235 -A	0.028
	EPCL235 -B	0.014
MPCL570	MPCL570-A	0.060
	MPCL570- B	0.030
YPCL570	YPCL570-A	0.022
	YPCL570- B	0.011
EPCL570	EPCL570- A	0.038
	EPCL570- B	0.019
MPCL235-P (Placebo)	MPCL235-P-A	Used at similar higher concentration of MPCL235 and MPCL570 dose.
MPCL570-P (Placebo)	MPCL570-P-A	

* Suffix A and B in formulation code represent half and quarter IC_{50} dose treatment respectively

Table 7.10 Subtoxic dose (Half and quarter IC_{50} value, 48 h incubation) of ETO and micellar formulations and their respective code used for *in vitro* cell line studies

7.4.2 Cytopathic study

Cytopathic assay was carried out to see the effect of plain ETO and micellar formulations on morphology of B16F10 cells after treatment with subtoxic concentration (half and quarter IC_{50} dose). Cells were stained with haematoxilin and eosin after incubation with micellar formulations for 48 h. As shown in Figure 7.9 to 7.14, it was observed that plain ETO and micellar formulation exhibited significant changes in cell morphology. Moreover, the changes in cell morphology were found

concentration dependent. Cells treatment with half IC_{50} dose showed more pronounced effect compared to quarter IC_{50} dose. A large number of dendrites and cell protrusions were observed in B16F10 cells after treatment with subtoxic concentrations of ETO and micellar formulations. Cells appeared spindle-shaped with some amount of hypertrophy as compared to control cells which were star-shaped and much more spread out. These observations are somewhat similar to earlier report with pentoxifyline on B16F10 cells (Dua & Gude, 2006).

Furthermore, B16F10 melanoma cells began to show cell shrinkage, rounding and fragmentation, thus changed the typical appearance of cells compare to untreated cells. B16F10 cells treated with placebo formulation showed no any change in cell morphology. Cancer cell have altered morphology compared to normal cells and these altered cell shapes contribute to increased cell movement seen in cancer cells. A direct consequence of this defect leads to migration and spreading of malignant cancer cells throughout the patient's body. Moreover, the shape and surface properties of cancer cells are commonly assumed to be related with their neoplastic character and their ability to produce metastasis (Wojciak & Korohoda, 1990). It is assumed that after treatment with micellar formulations, the change in morphology of cancer cell observed might help in prevention of cell migration and metastasis to distant sites.

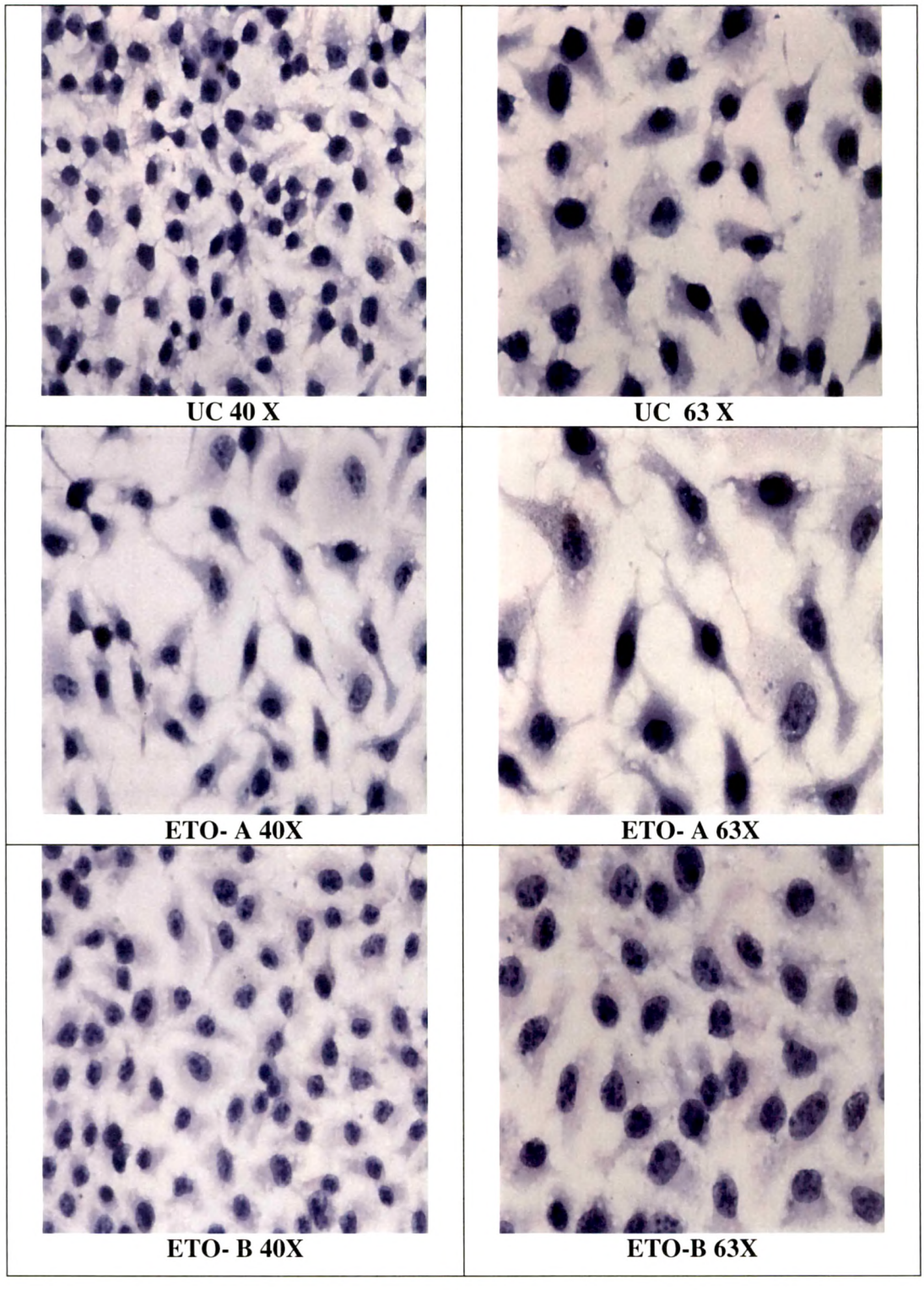

Figure 7.9 Morphological changes of B16F10 cells after treatment with ETO and morphological image of untreated control (UC)

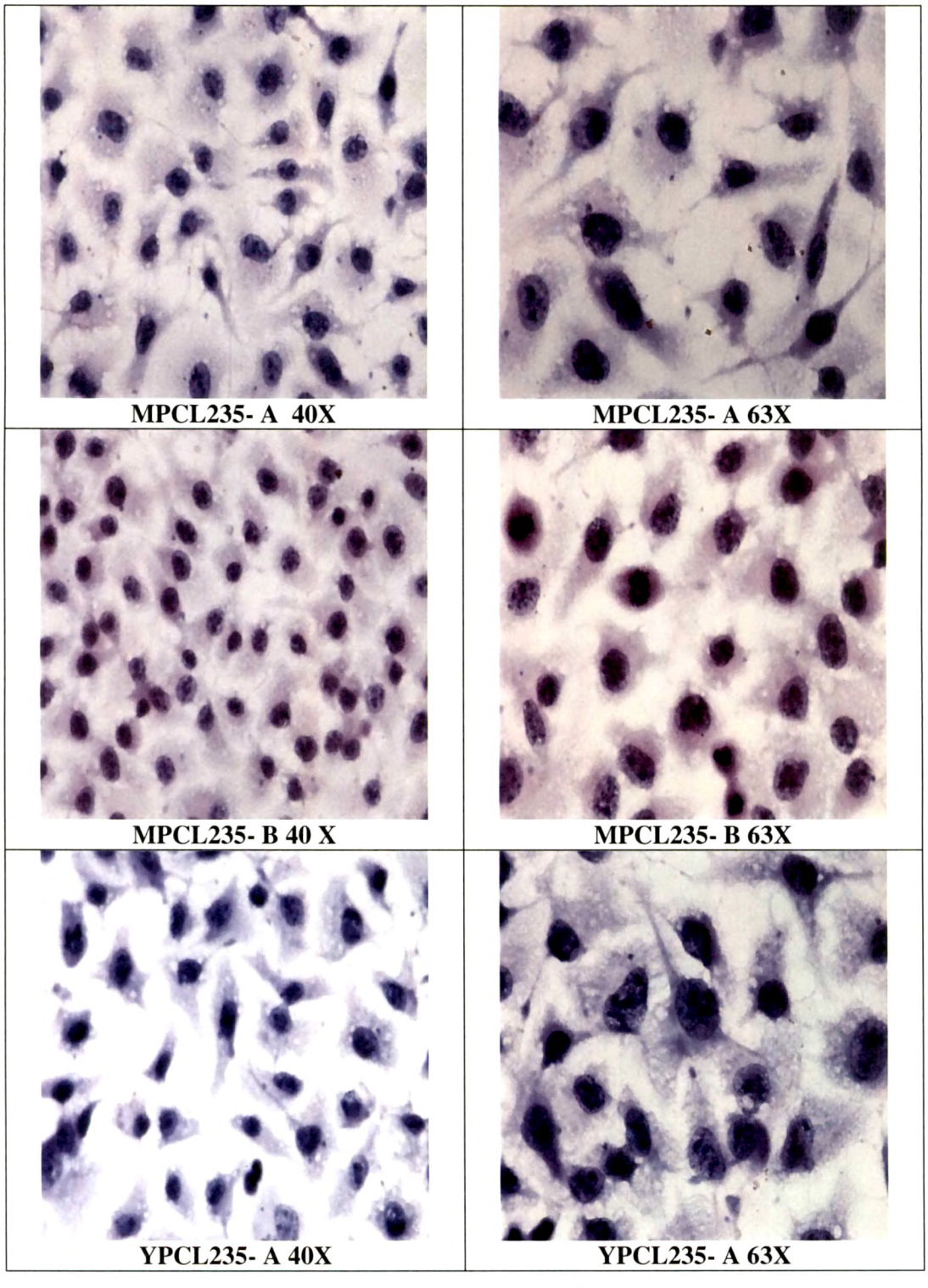

Figure 7.10 Morphological changes of B16F10 cells after treatment with MPCL235 and YPCL235

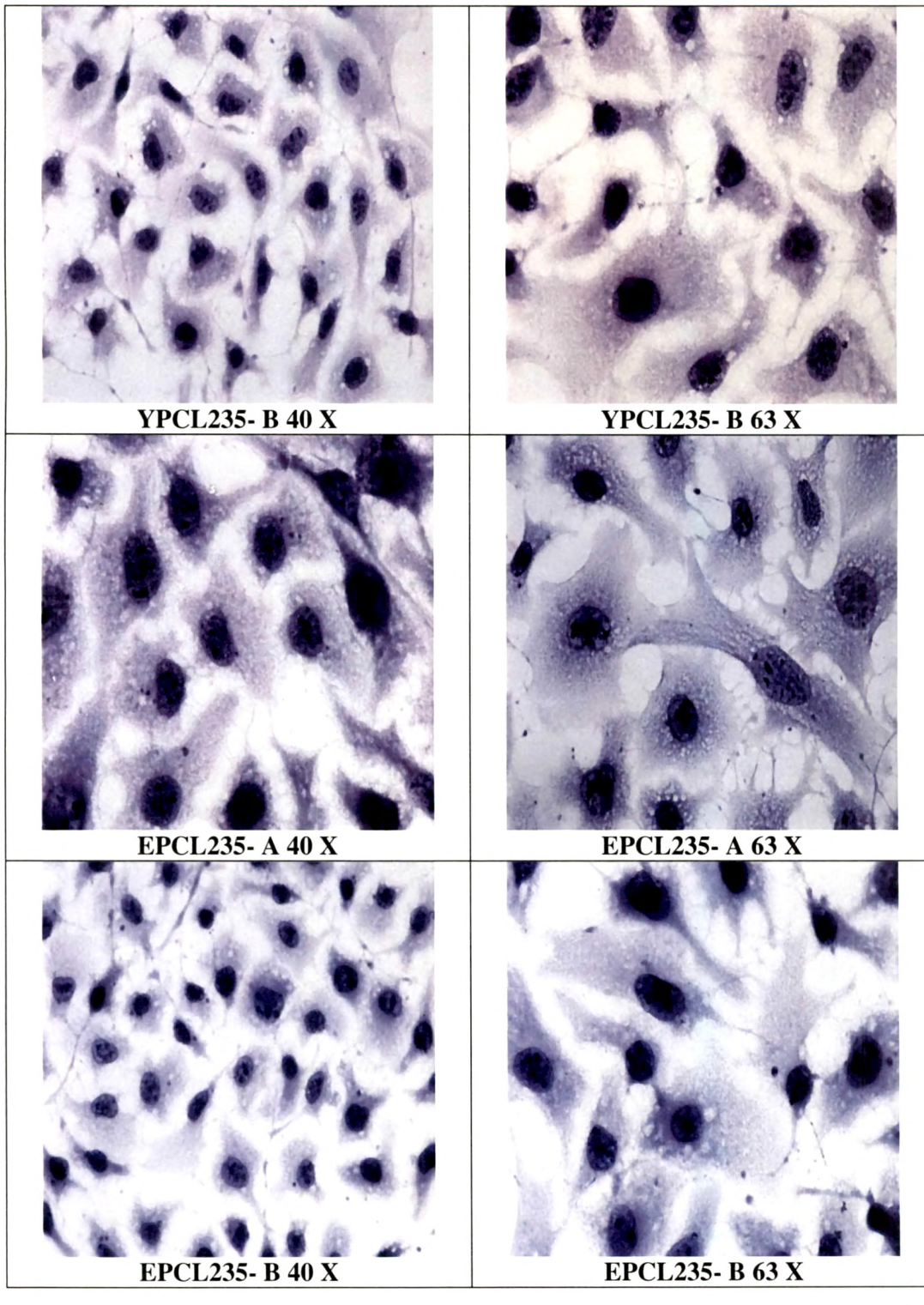

Figure 7.11 Morphological changes of B16F10 cells after treatment with YPCL235 and EPCL235

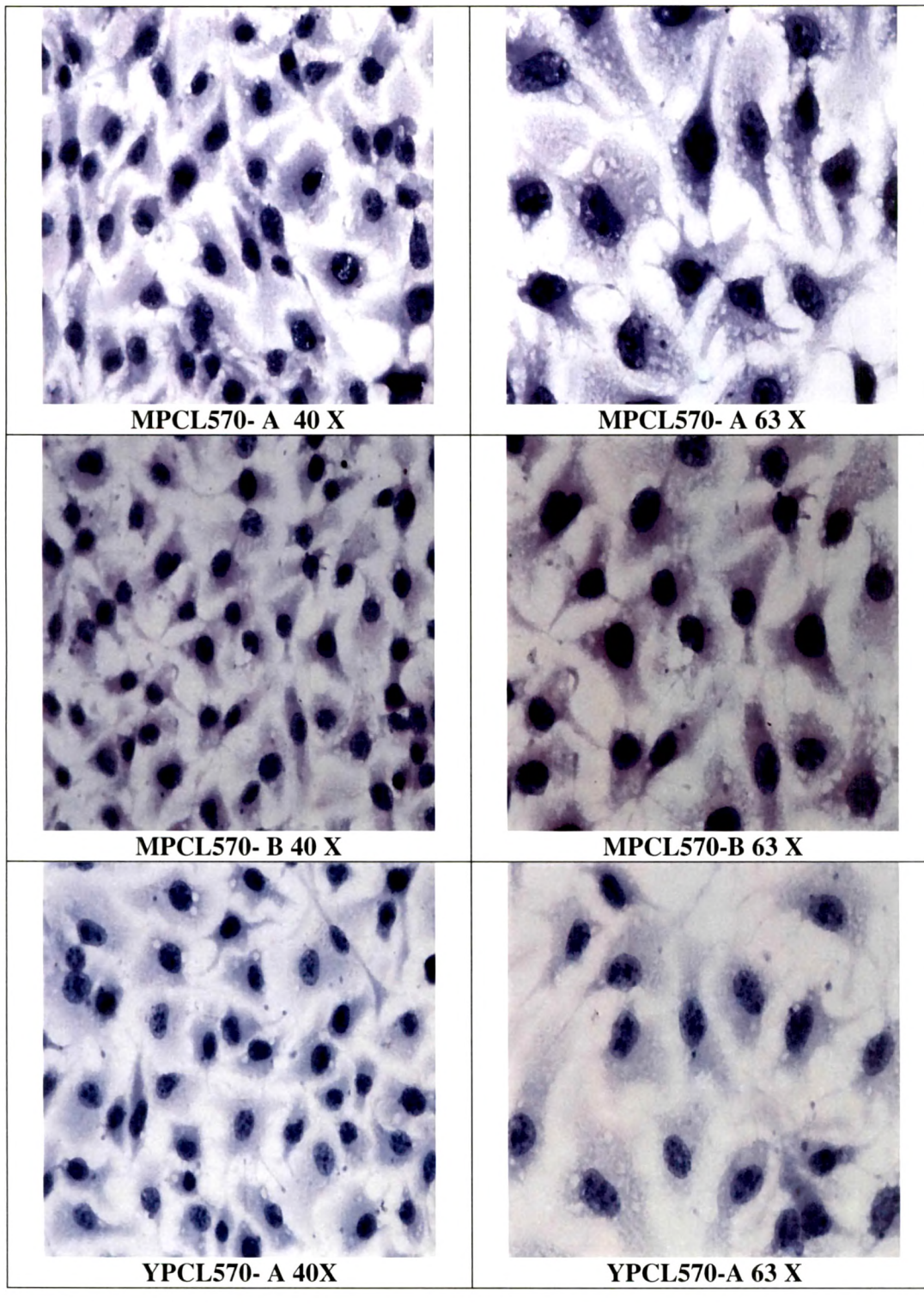

Figure 7.12 Morphological changes of B16F10 cells after treatment with MPCL570 and YPCL570

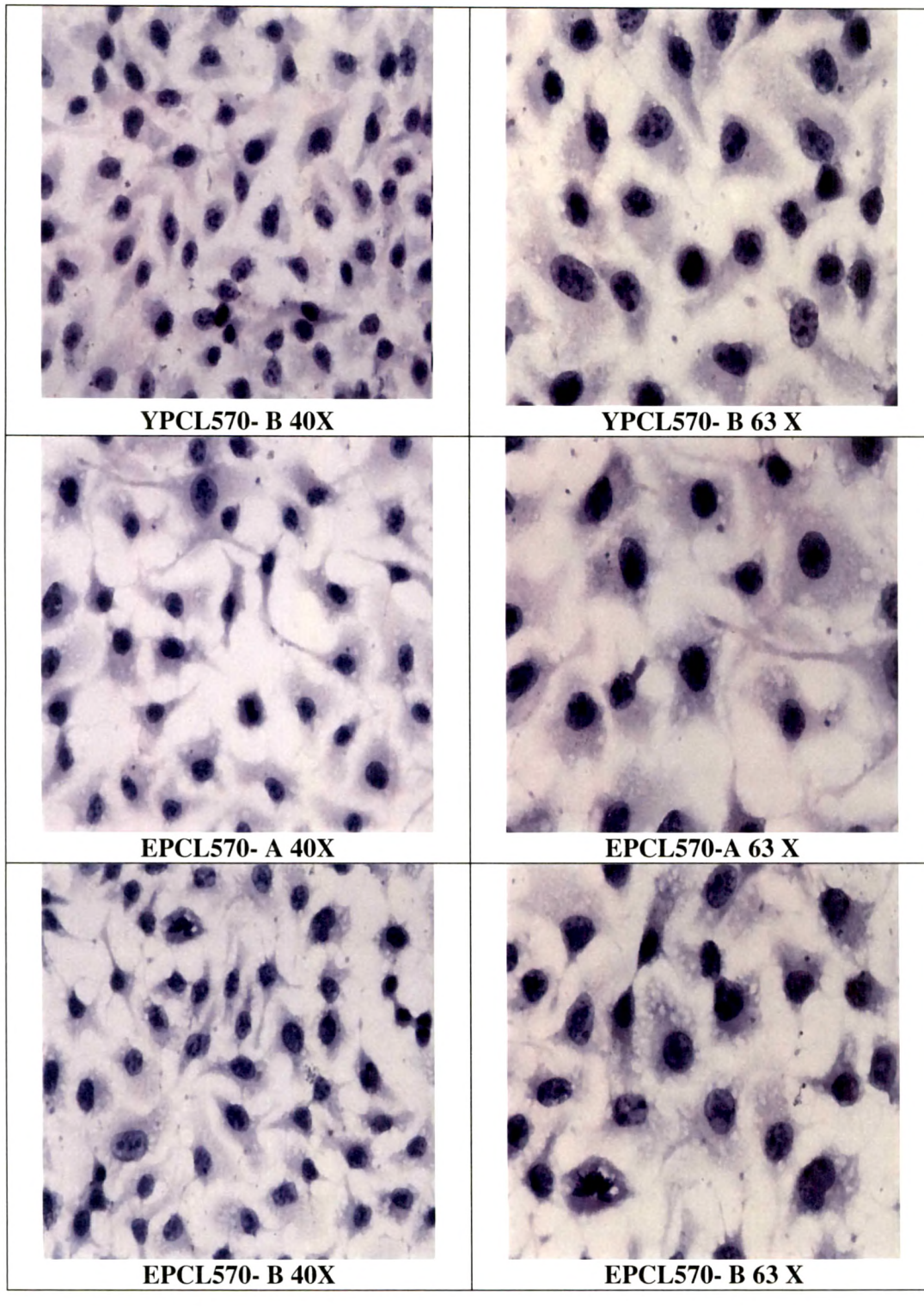

Figure 7.13 Morphological changes of B16F10 cells after treatment with YPCL570 and EPCL570

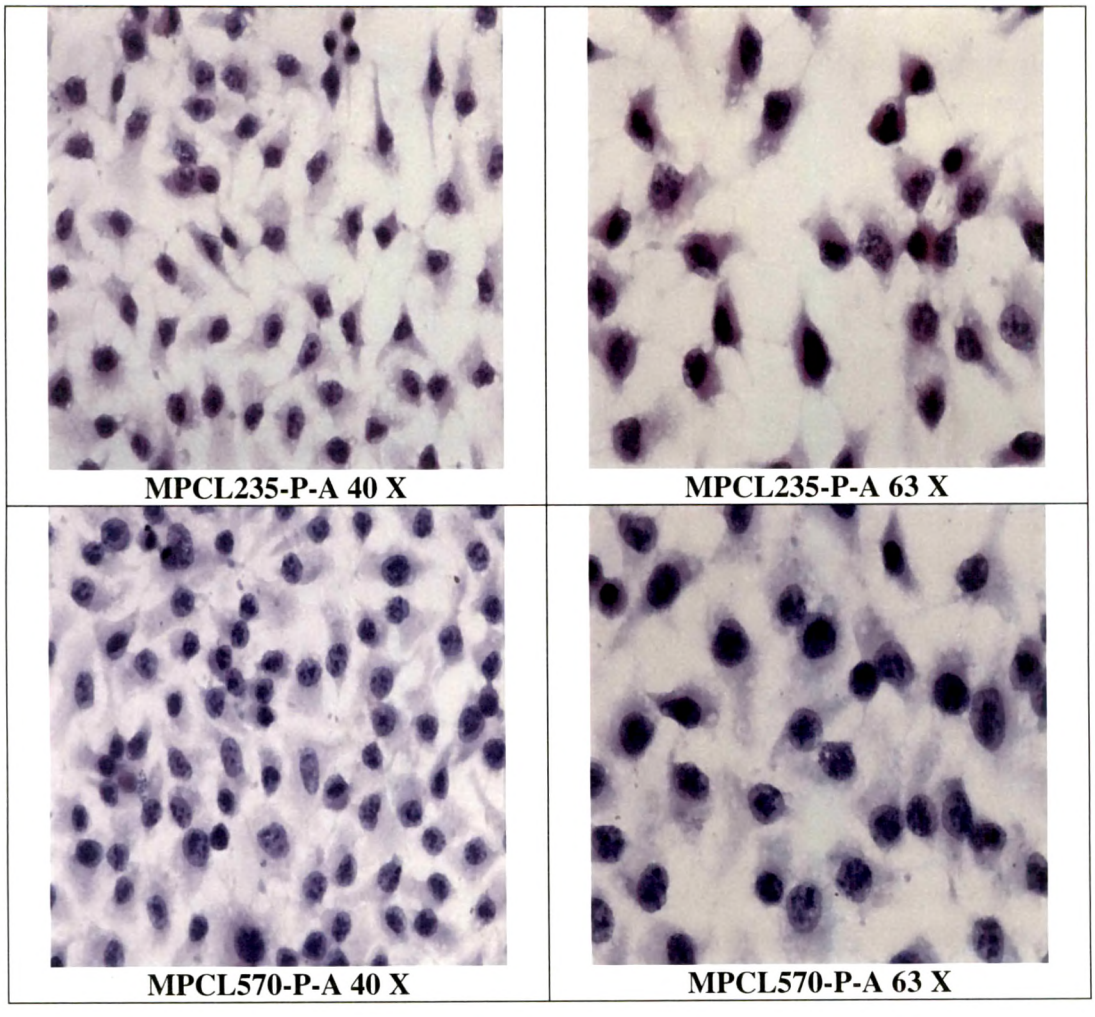

Figure 7.14 Morphological changes of B16F10 cells after treatment with MPCL235-P and MPCL570- P

7.4.3 Colony forming assay

The colony formation assay (CFA) is the gold standard for measuring the effects of cytotoxic agents on cancer cells *in vitro* (Katz et al., 2008). The assay essentially tests every cell in the population for its ability to undergo ''unlimited'' division and is the method of choice to determine cell reproductive death after cytotoxic agents treatment or ionizing radiation (Franken et al., 2006). Colony formation assay of plain ETO and micellar formulations were carried out incubating cell with half and quarter dose of IC_{50} values (48 h) and after completion of experiment, the numbers of colonies having more than 50 cells were counted. Figure 7.15 shows the images of colonies formed of B16F10 cells.

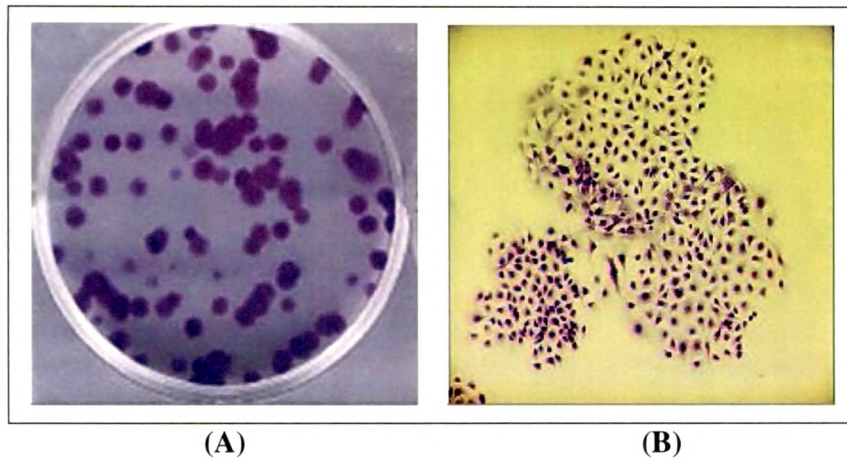

(A) **(B)**

Figure 7.15 Typical images of colony formation, where A and B represents the complete image of colonies in plate and individual colonies with more than 50 cells

The percent colony inhibition of B16F10 cells after treatment with plain ETO and micellar formulations with respect to control is represented in Table 7.11 and Figure 7.16 & 7.17. It was observed that all formulation exhibited inhibitory effect on colonization of B16F10 cells and the effect was concentration dependent. In all formulations, maximum inhibition in colony formation was found at half IC_{50} concentration compared to quarter IC_{50} dose treatment. Plain ETO at half and quarter IC_{50} dose showed 42.07 ± 2.80 and 29.0 ± 7.36 percent colony inhibition respectively, which was lesser, compared to all micellar formulations and reflects the results obtained in cytotoxicity studies. Peptide YIGSR conjugated micelles YPCL235 and YPCL570 showed higher inhibition in colony formation compared to non conjugated micelles MPCL235 and MPCL570 (Table 7.11). A comparison of two peptide

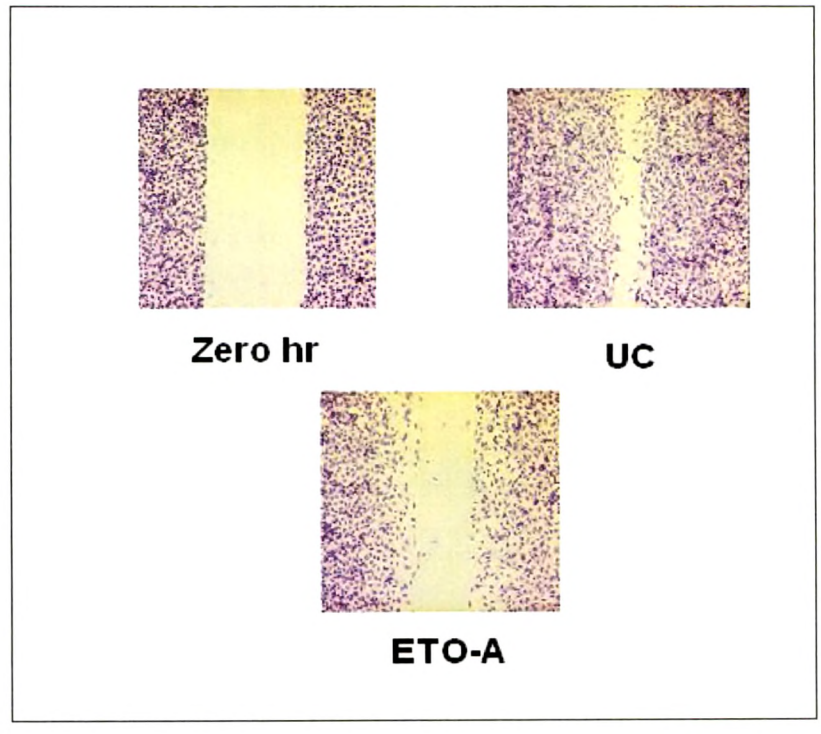

Figure 7.18 Microscopic wound images of Zero h reference plate, Untreated control and Plain ETO-A

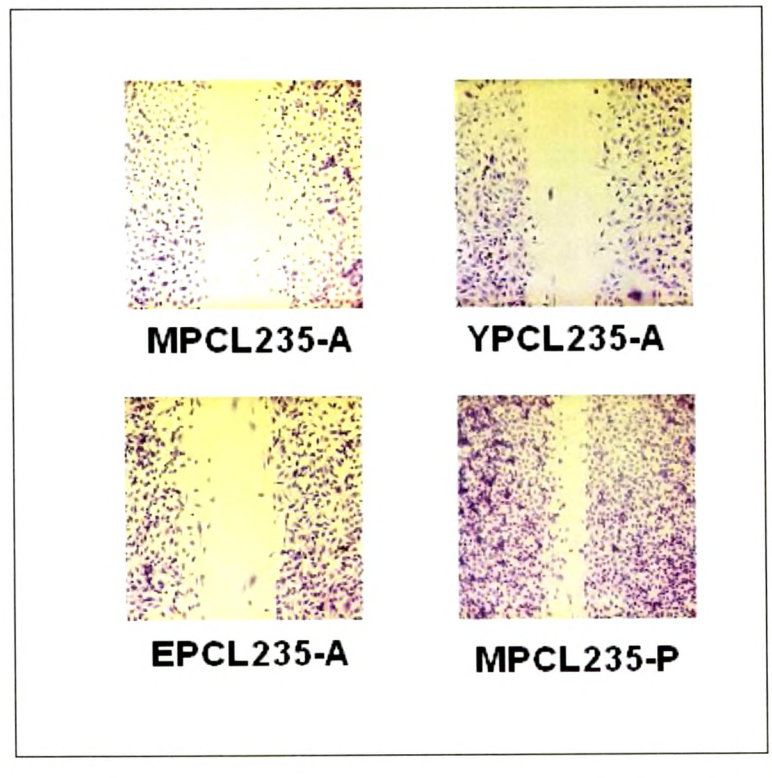

Figure 7.19 Microscopic wound images of MPCL235-A, YPCL235-A, EPCL235-A and MPCL235-P-A

conjugated micelles (i.e. with YIGSR-NH_2 and EILDV-NH_2), YIGSR-NH_2 conjugated micelles YPCL235 and YPCL570 showed little more potent effect compared to EPCL235 and EPCL570. Compared to plain ETO, micellar formulations exhibited higher inhibition in colony formation, due to sustained release of drug from the micelles internalized into cell even after completion of incubation period. Since in experiment, cells were washed 48 h after drug treatment and incubated further for 48 h and during these time period the internalized micelles released drug slowly. The presence of higher amount intracellular drug released from micelles might have slow down the colonization of B16F10 cells compared to plain ETO. Blank formulation were also tested and showed no inhibition in colony formation. A group of Woo and his colleagues investigated the effect of deguelin incorporated liposomes using NSCLC cell lines (Woo et al., 2009) and reported that deguelin loaded liposomes significantly inhibited the anchorage independent colony forming abilities of NSCLC cell lines compared to plain deguelin.

Formulation code	**% Inhibition in colony formation**	**Formulation code**	**% Inhibition in colony formation**
ETO- A	42.07 ± 2.80	MPCL570-A	48.46 ± 8.71
ETO- B	29.00 ± 7.36	MPCL570- B	36.35 ± 7.79
MPCL235-A	52.86 ± 6.22	YPCL570-A	60.58 ± 10.90
MPCL235-B	37.45 ± 5.60	YPCL570- B	42.51 ± 7.16
YPCL235-A	63.88 ± 1.86	EPCL570- A	59.47 ± 3.74
YPCL235-B	43.39 ± 2.80	EPCL570- B	42.29 ± 4.98
EPCL235-A	58.37 ± 5.29	MPCL235-P-A	5.08 ± 9.02
EPCL235-B	40.97 ± 4.98	MPCL570-P-A	3.75 ± 8.41

Table 7.11 Percent colony inhibition of B16F10 cells after treatment with subtoxic dose of plain ETO and micellar formulations (The experiments were conducted thrice and the results are mean ± S.D.)

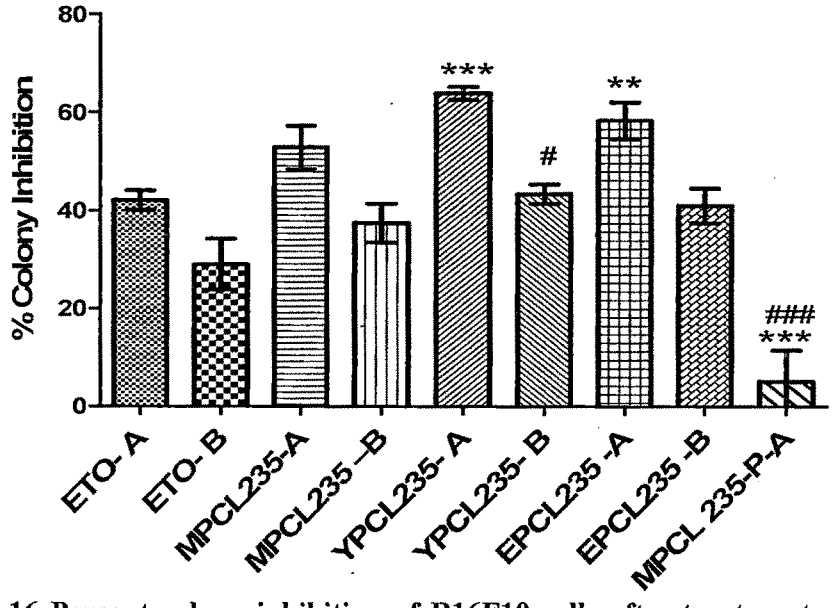

Figure 7.16 Percent colony inhibition of B16F10 cells after treatment with two subtoxic doses of ETO, MPCL235, YPCL235, EPCL235 and MPCL235-P-A (The * and ** indicates P<0.001 and P<0.01 compared to ETO-A, while ### and # indicates P<0.001 and P<0.05 compared to ETO-B)**

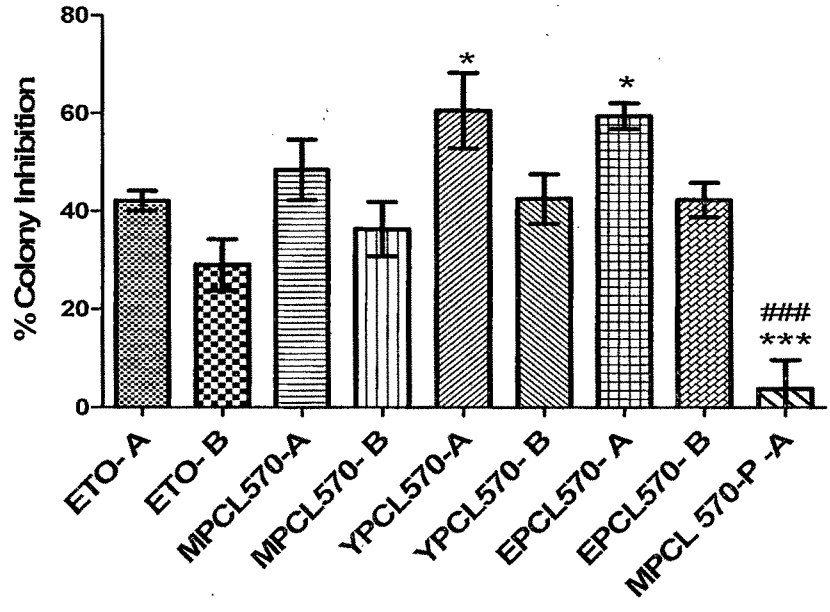

Figure 7.17 Percent colony inhibition of B16F10 cells after treatment with two subtoxic doses of ETO, MPCL570, YPCL570, EPCL570 and MPCL570-P-A (The * and * indicates P <0.001 and P<0.05 compared to ETO-A, while ### indicates P<0.001 compared to ETO-B)**

7.4.4 Cell migration assay

Metastases kill 90% of cancer patients. It is thus a major challenge in cancer therapy to inhibit the spreading of tumor cells from primary tumor sites to those particular organs where metastases are likely to occur. Hence, compounds that can interfere with such process are clinically important. Tumor cell migration was evaluated by scratch wound assay model. There are various methods reported for evaluation of tumor cell migration like *in vitro* scratch assay, boyden chamber method and microfluidics based system (Liang et al., 2007). However, the *in vitro* scratch assay method is a simple and inexpensive method compared to other method. This method is based on the observation that, upon creation of a new artificial gap, so called "scratch", on a confluent cell monolayer, the cells on the edge of the newly created gap will move toward the opening to close the "scratch" until new cell–cell contacts are established again.

The cell migration of B16F10 cells after treatment with ETO and micellar formulations at two subtoxic concentrations i.e. IC_{25} and $IC_{12.5}$ showed their potential in prevention of cell migration and the effect was concentration dependent (Table 7.12). Figure 7.18 to 7.20 represents the microscopic wound images of zero h reference plate, untreated control and formulation treated with IC_{25} dose plates.

Formulation Code	% Cell Migration	Formulation Code	% Cell Migration
UC	100.00	MPCL570-A	33.24 ± 8.42
ETO-A	41.92 ± 3.97	MPCL570-B	63.15 ± 2.96
ETO-B	55.04 ± 5.98	YPCL570-A	25.67 ± 5.06
MPCL235-A	32.33 ± 6.23	YPCL570-B	69.57 ± 3.62
MPCL235-B	55.15 ± 4.20	EPCL570-A	21.73 ± 6.67
YPCL235-A	24.86 ± 8.57	EPCL570-B	67.48 ± 10.18
YPCL235-B	45.21 ± 6.63	MPCL235-P-A	97.16 ± 9.89
EPCL235-A	28.91 ± 5.53	MPCL570-P-A	98.31 ± 5.64
EPCL235-B	56.51 ± 3.86		

Table 7.12 Percent cell migration of B16F10 cells after treatment with plain ETO, non conjugated micelles and peptide conjugated micelles (The results are mean ± S.D. of three individual experiments and percent cell migration was considered compared to migration of untreated control B16F10 cells as 100 %)

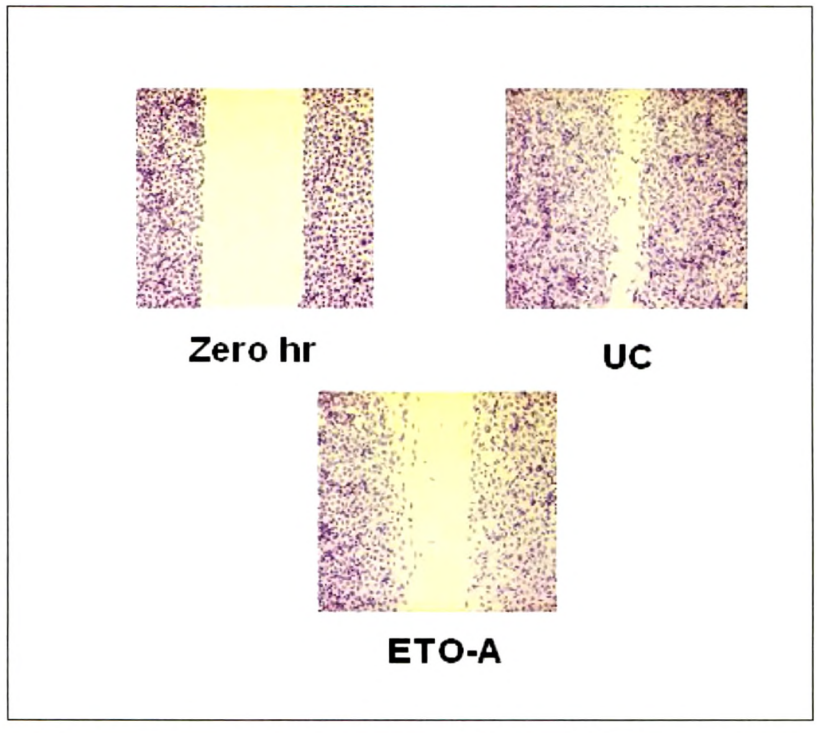

Figure 7.18 Microscopic wound images of Zero h reference plate, Untreated control and Plain ETO-A

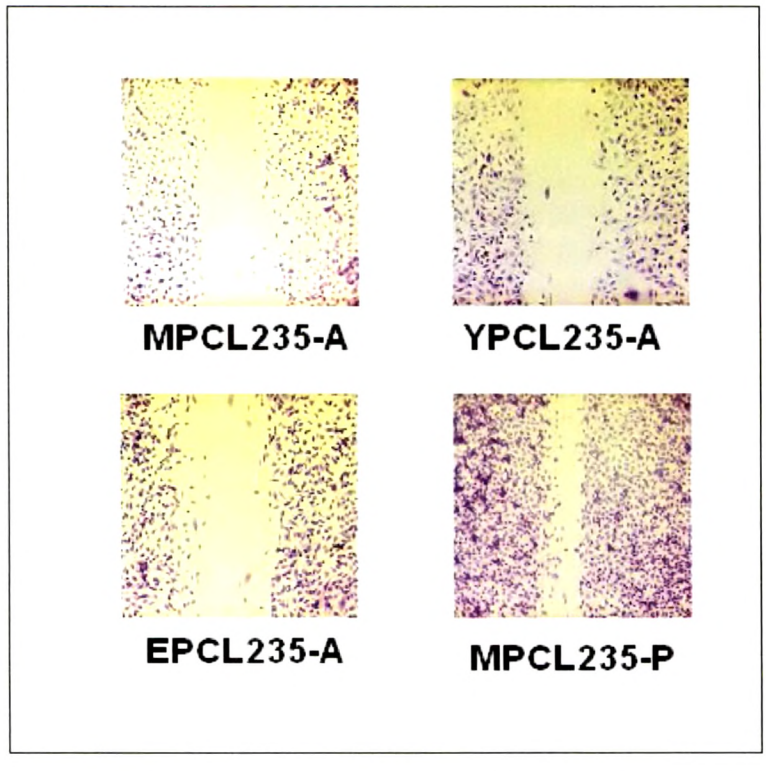

Figure 7.19 Microscopic wound images of MPCL235-A, YPCL235-A, EPCL235-A and MPCL235-P-A

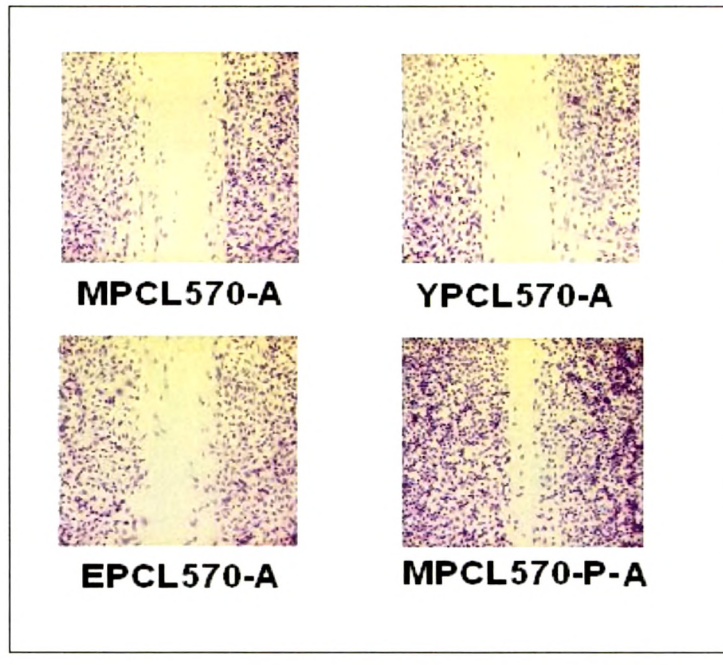

Figure 7.20 Microscopic wound images of MPCL570-A, YPCL570-A, EPCL570-A and MPCL570-P-A

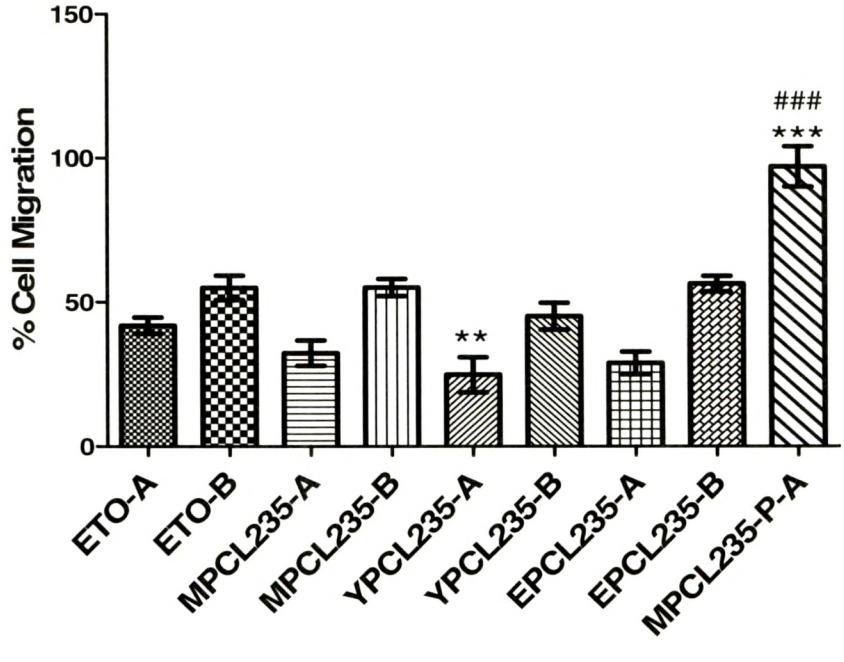

Figure 7.21 Percent cell migration of B16F10 cells treated with ETO, MPCL235, YPCL235, EPCL235 and MPCL235-P (The * and ** indicates P<0.001 and P<0.01 compared to ETO-A, while ### indicates P<0.001 compared to ETO-B**

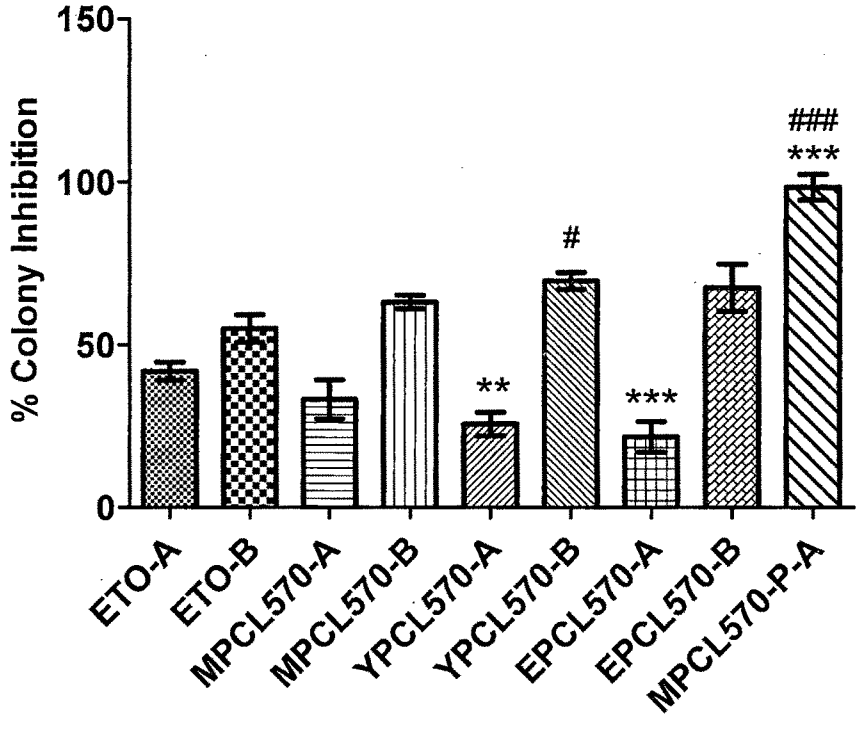

Figure 7.22 Percent cell migration of B16F10 cells treated with ETO, MPCL570, YPCL570, EPCL570 and MPCL570-P (The * and ** indicates P<0.001 and P<0.01 compared to ETO-A, while ### and # indicates P<0.001 and P<0.05 compared to ETO-B)**

Zero h plate was used as reference plate for calculation of percent cell migration. To evaluate only the migratory effect and not the proliferative effect of B16F10 cells, after wound creation media was used containing only 0.1% serum. In untreated control, the average measured wound width was 95.14 micrometer compared to zero h plate wound width 311.36 micrometer and covered the wound upto 70 %. Considering the untreated control cell migration as 100 percent, the percent cell migration of plain and micellar formulations treated B16F10 cells were calculated and represented in Table 7.12. It was shown that as compared to plain ETO, all micellar formulations showed higher inhibition in cell migration (Figure 7.21 & 7.22). Moreover, the peptide tagged micellar formulation exhibited more pronounced effect compared to non conjugated micelles. In YPCL235-A treated formulation, the percent cell migration found was 24.86 ± 8.57 while EPCL235-A showed percent cell migration of 28.91 ± 5.53. Same way YPCL570-A showed 25.67 ± 5.06 and EPCL570-A showed 21.73 ± 6.67 percent cell migration. The results obtained clearly indicates that

peptide conjugated micellar formulation have more potential towards prevention of migration of cell. Placebo micellar formulations showed no any effect on cell migration as shown in microscopic images taken (Figure 7.21 and 7.22)

Cell movement through tissue plays an important and primary role in cancer progression. This process requires a series of distinct but concerted biological events in which the actin cytoskeleton plays essential roles. These include tumor cell attachment to the extracellular matrix (ECM) components, the degradation of the matrix by tumor cell-associated proteases, and tumor cell progression into the region where the matrix is modified by proteolysis (Hayot et al., 2006). Observation from cytopathic studies has shown that ETO can change the morphology of tumor cell as well the cytoskeleton of cell. It is also known that migrating cells show decreased proliferation rate and are thus less sensitive to standard chemotherapy (Douma et al., 2004; Lefranc et al., 2005). In the advance treatment of cancer, it is now required to inhibit or, at least to reduce, the spreading of tumor cells by targeting the factors which can regulate the migratory activity of these cells, and so to prevent metastasis. In this juncture, peptide like YIGSR-NH_2 and EILDV-NH_2 that interfere with tumor cell adhesion to ECM compounds if conjugated to surface of polymeric micelles loaded anticancer drug, possibly give an additional benefit in prevention of cell migration because of their antimetastatic properties. However, peptide EILDV-NH_2 and YIGSR-NH_2 was reported to have antimigratory effect but required large dose to exert this effect with an issue of its in vivo stability (Murata et al., 1989; Yoshihisa et al., 1997).

7.4.5 Cell adhesion study

The aim of this study was to investigate the native inherent adhesive property of peptide after conjugation as well as the ability of cell adhesion of B16F10 cells to substrate after drug treatment. The study was carried out using YIGSR-NH_2 and EILDV-NH_2 as substrate instead of laminin and fibronectin based on reports by Yamamura et al. (1993). Since, the adhesion of tumor cells to ECM is essential for metastasis (Dua et al., 2007). It is reported that B16F10 cells have expression of laminin and integrin receptors and this receptor helps in binding of cells to extracellular matrix proteins or peptides sequence (derived from ECM proteins) responsible for cell adhesions (Engbring et al., 2002; Ratheesh et al., 2007).

Formulation code	YIGSR-NH_2 coated plate	EILDV-NH_2 coated plate
	% Cell adhesion	% Cell adhesion
Uncoated wells	100.00 ± 5.04	100.00 ± 7.63
ETO	71.46± 5.91	66.30 ± 5.27
MPCL235-A	64.00 ± 9.68	54.84 ± 6.37
YPCL235-A	27.19 ± 7.75	----
EPCL235-A	----	38.27 ± 9.66
MPCL570-A	58.52 ± 8.15	61.96 ± 8.67
YPCL570-A	31.06 ± 2.87	----
EPCL570-A	----	40.73 ± 4.90
MPCL235-P-A	87.31 ± 7.80	81.88 ± 3.52
MCPL570-P-A	93.47 ± 6.33	91.55 ± 2.57

Table 7.13 Percent cell adhesion of B16F10 cells after treatment with micellar formulation against YIGSR-NH_2 and EILDV-NH_2 coated plate (The results are mean ± S.D. and n=3)

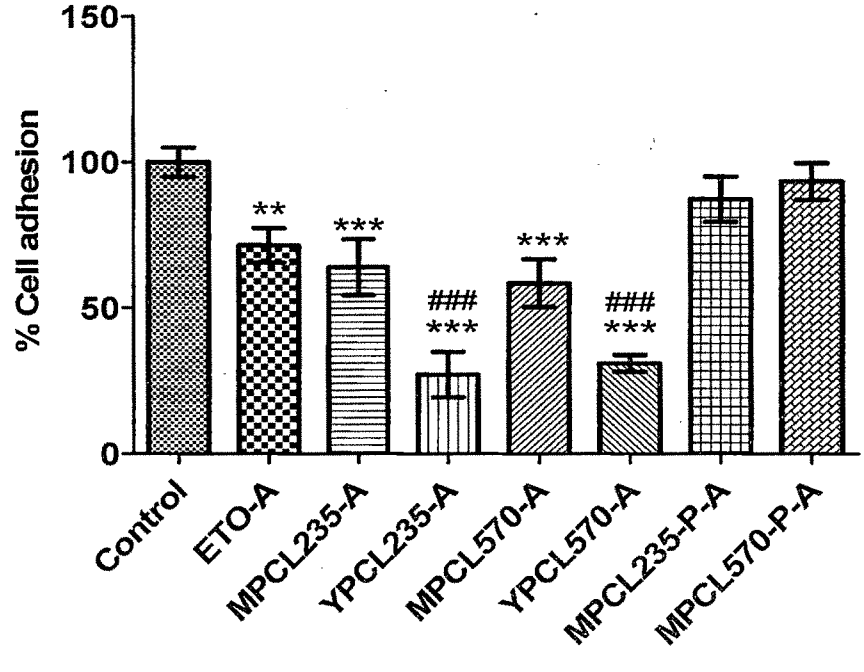

Figure 7.23 Percent cell adhesion of B16F10 cells after treatment with micellar formulation to YIGSR-NH_2 coated plate (* and ** indicates P<0.001 and P<0.01 compared to control (uncoated well), while ### indicates P<0.001 compared to ETO-A)**

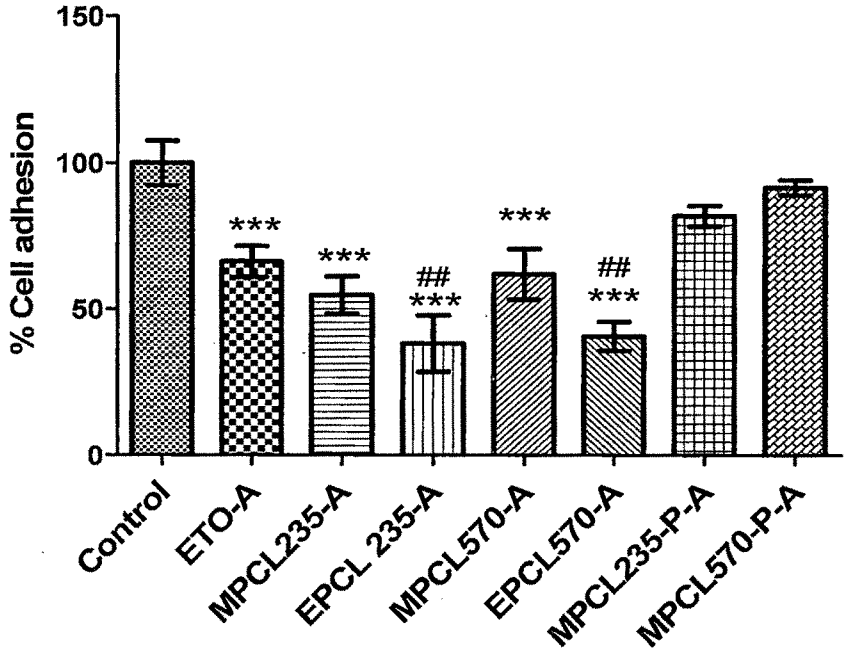

Figure 7.24 Percent cell adhesion of B16F10 cells after treatment with micellar formulation to EILDV-NH_2 coated plate (* indicates P<0.001 compared to control (uncoated well), while ### and ## indicates P<0.001 and P<0.01 compared to ETO-A).**

YIGSR-NH_2 or EILDV-NH_2 was used as substrate and the percent cell adhesion was calculated with reference to adhesion of uncoated well. The results obtained are represented in Table 7.13 and Figure 7.23 & 7.24. As compared to control (uncoated well), ETO and all micellar formulation treated B16F10 cells showed a significant inhibition cell adhesion in both the substrate coated plates. The results obtained suggest that after subtoxic dose treatment with ETO and micellar formulations, cell adhesion of B16F10 cells to substrate reduced significantly which could be helpful in prevention of metastasis. YPCL235-A and YPCL570-A exhibited minimum cell adhesion of 27.19 ± 7.75 & 31.06 ± 2.87 percent with significant difference (P<0.001) to ETO-A. Same way, EILDV conjugated micelles EPCL235-A and EPCL570-A exhibited percent cell adhesion of 38.27 ± 9.66 & 40.73 ± 4.90 respectively with significantly difference (P< 0.001) compared to ETO-A. A two fold reduction in cell adhesion was observed with YIGSR conjugated micelles compared to non conjugated micelles while EILDV conjugated micelles showed nearly 1.5 fold reduction in cell adhesion to that of non conjugated micelles. The significant difference observed in cell adhesion of peptide conjugated micelles to that of plain ETO implies that

conjugated peptide plays a major role in cell adhesion process. It was assumed that during treatment of B16F10 cells with peptide conjugated micelles, the micelles after receptor recognition internalized into cell and the process remained continued till total depletion of micelles outside the cells. These process leads to availability of very few laminin and integrin receptors on the surface of B16F10 cells which is required to attach to substrate. The obtained data clearly suggest that both the peptide after conjugation to micelles retained their inherent adhesive properties. The results obtained are in agreement with study carried out using YIGSR tagged liposomes by Lopez et al. (2004), who reported that YIGSR was functionally active even after conjugation to the surface of PEG based liposomes and inhibited cell adhesion to laminin coated plates.

7.4.6 Confocal microscopy

It is clear that therapeutic effects of drug loaded micelles or nanoparticles would depend upon the internalization and sustained retention of the nanoparticles in diseased cells. A confocal microscopy was performed to find out the uptake of non-conjugated and peptide conjugated micellar formulation loaded with fluorescent dye 6-coumarin. Previous studies have demonstrated that 6-coumarin can be used as dye for cellular uptake of nanoparticles (Davda & Labhasetwar, 2002; Panyam et al., 2003). Moreover, it was also reported that less than 0.6 % incorporated dye can leach out from nanoparticles over 48 h under *in vitro* sink conditions, means the dye could not leach from the micelles during the experimental time frame and hence the fluorescence seen in the cells is caused by micelles and not by dye (Desai et al., 1997).

Cellular uptake studies of 6-coumarin loaded micellar formulations were carried out at 1 h and 3 h incubation and the images obtained are represented in Figure 7.25 & 7.26. Comparing the confocal images of 1 h and 3 h, it was deduced that the cellular uptake was depend on time of incubation and stronger fluorescence intensity was observed at 3 h incubation. The study also supports the receptor based internalization of peptide conjugated micelles which generally have enhanced cellular uptake. In Figure 7.25 & 7.26, the fluorescence intensity was more enhanced in peptide conjugated micelles YPCL235, EPCL235, YPCL570 and EPCL570 compared to MPCL235 and MPCL570, implies active internalization of peptide conjugated micelles (Acharya et al., 2009).

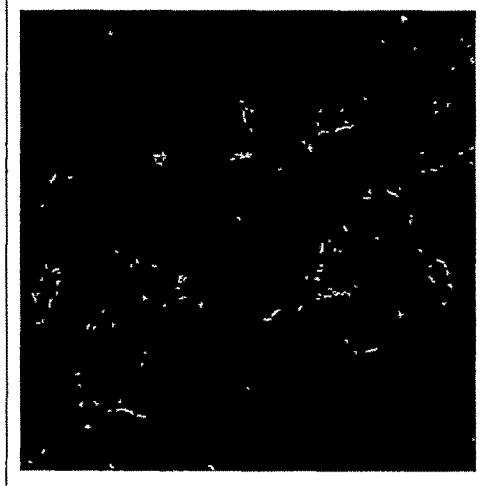

MPCL235 1 h

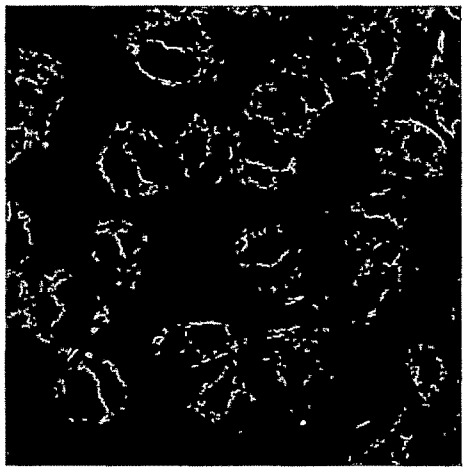

MPCL235 3 h

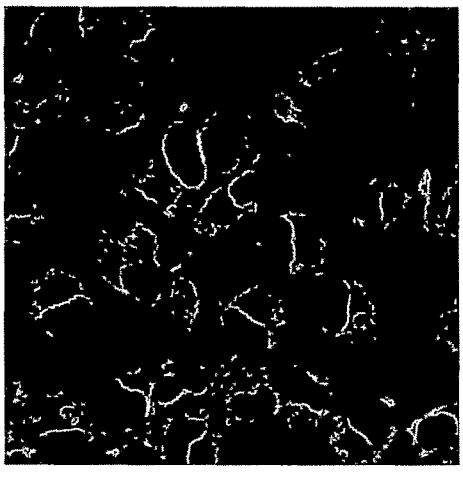

YPCL235 1 h

YPCL235 3 h

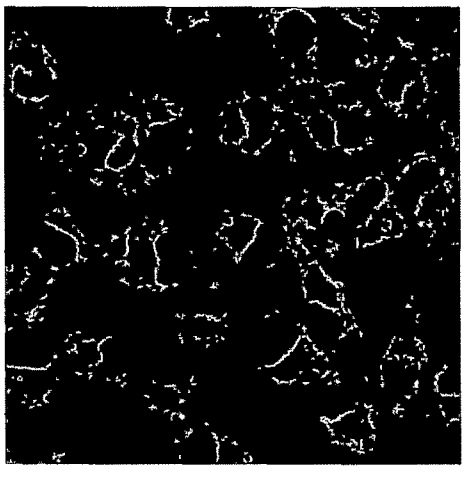

EPCL235 1 h

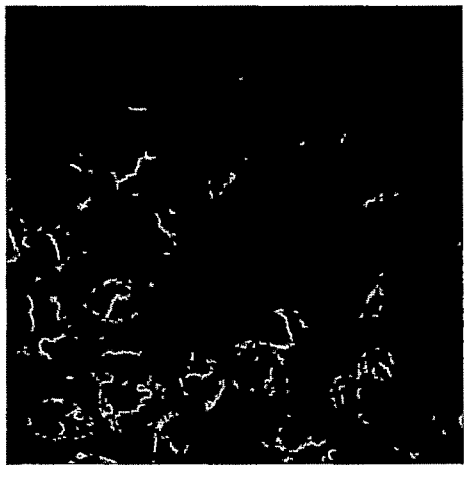

EPCL235 3 h

Figure 7.25 Confocal fluorescence images of MPCL235, YPCL235 and EPCL235 micelles (loaded with 6-Coumarin) after incubation of 1 and 3 h

MPCL570 1h

MPCL570 3 h

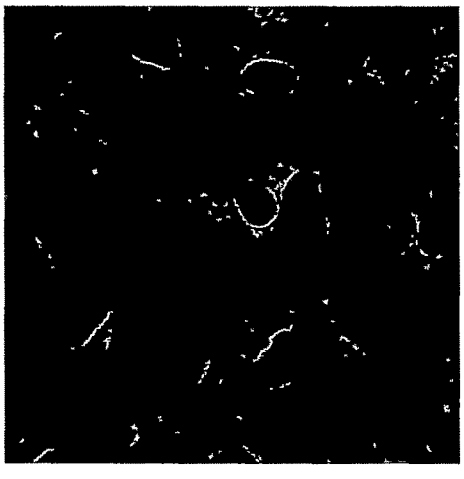

YPCL570 1 h

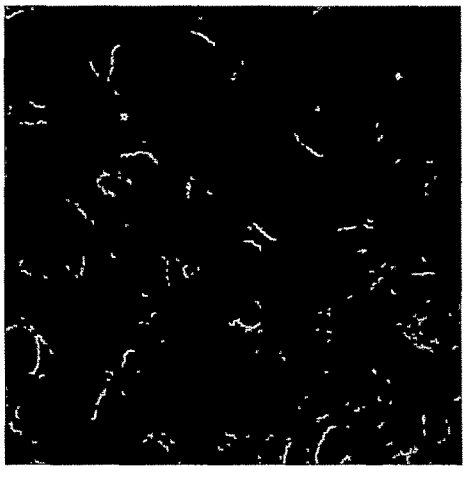

YPCL570 3 h

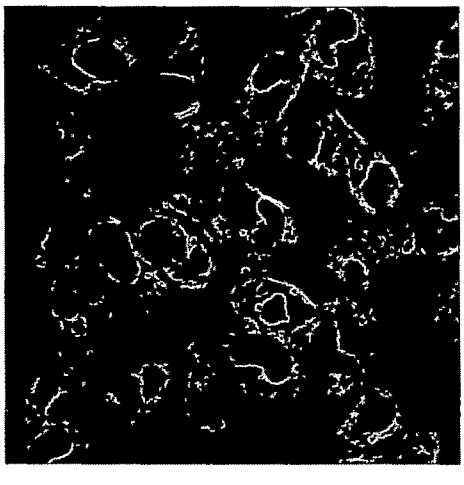

EPCL570 1h

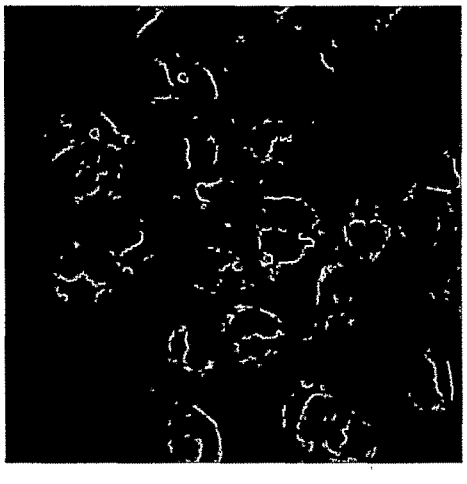

EPCL570 3 h

Figure 7.26 Confocal fluorescence images of MPCL570, YPCL570 and EPCL570 micelles (loaded with 6-Coumarin) after incubation of 1 and 3 h

7.4.7 Cell uptake studies

The amount of ETO accumulated in B16F10 cells after incubation of ETO and micellar formulations was determined by reverse phase HPLC method. B16F10 cells were incubated for 2 h at drug concentration of 20 µg/ml and washed with cold PBS in order to remove cell membrane adhered free ETO and micelles. It is important to know the effect of surface density of peptide on the internalization of micelles. Peptide YIGSR-NH_2 or EILDV-NH_2 was conjugated on the surface of micelles at different surface density i.e. 5 %, 10 % and 20 % preparing micelles with different ratio of functionalized to non functionalized polymer. Table 7.14 and Figure 7.27 & 7.28 represent the percent cellular uptake of etoposide from plain ETO and micellar formulations measured by HPLC method.

Formulation code	Percent cellular uptake of drug	Formulation code	Percent cellular uptake of drug
ETO	75.02 ± 5.23	MPCL570	5.30 ± 1.51
MPCL235	6.43 ± 2.81	YPCL570 [5 %]	9.31 ± 1.84
YPCL235 [5 %]	11.01 ± 2.98	YPCL570 [10 %]	13.30 ± 2.62
YPCL235 [10 %]	16.76 ± 2.15	YPCL570 [20 %]	16.54 ± 3.28
YPCL235 [20 %]	18.92 ± 3.01	EPCL570 [5 %]	8.09 ± 2.10
EPCL235 [5 %]	9.22 ± 1.36	EPCL570 [10 %]	13.28 ± 1.06
EPCL235 [10 %]	13.11 ± 2.67	EPCL570 [20 %]	15.76 ± 3.87
EPCL235 [20 %]	16.18 ± 2.40		

Table 7.14 Percent cellular uptake of drug by B16F10 cells after incubation of ETO and ETO loaded micelles for 2 h. Values in bracket indicates percent surface density of peptide YIGSR-NH_2 or EILDV-NH_2

It was observed that plain ETO after incubation of 2 h resulted into 75.02 ± 5.23 percent cellular drug uptake. The higher uptake of plain ETO was attributed due to its solubilized state of drug which resulted into rapid diffusivity of drug through cell membrane inside cells. The results obtained, supports the higher cytotoxicity exhibited by ETO at 24 h incubation. The non conjugated micelles MPCL235 and MPCL570 showed a percent cellular drug uptake of 6.43 ± 2.81 and 5.30 ± 1.51 respectively. A very low cellular uptake was observed with MPCL235 and MPCL570 compared to plain ETO due to its different route cell internalization (Table 7.14).

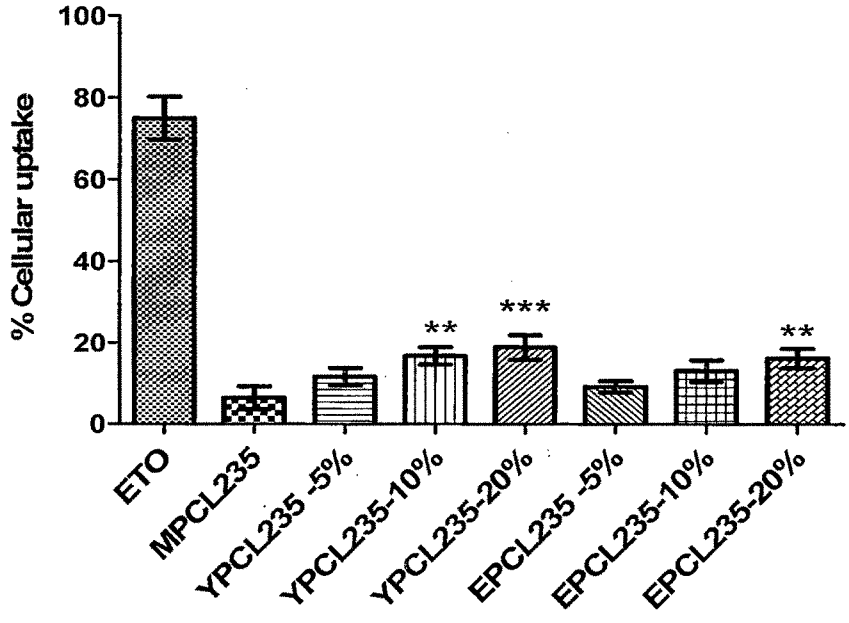

Figure 7.27 Percent cellular uptake of ETO, MPCL235, YPCL235 and EPCL235. The peptide conjugated micelles was formulated with different surface density of peptides (The ** and * indicates P<0.01 and P< 0.001 compared to MPCL235)**

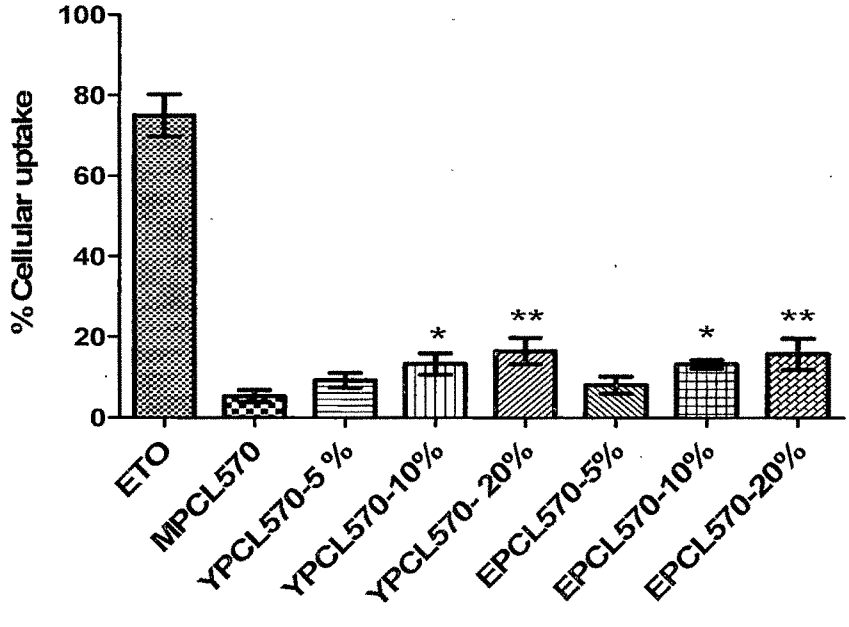

Figure 7.28 Percent cellular uptake of ETO, MPCL570, YPCL570 and EPCL570 micelles. The peptide conjugated micelles was formulated with different surface density of peptides (* and ** indicates P<0.05 and P<0.01 compared to MPCL570)

Luo et al. (2002) reported rhodamine conjugated PEG-PCL micelles internalization by endocytosis and it depends on various factor like pH, temperature, calcium ion concentration as well type of drug. Moreover, cellular internalization also depends on the particle size and charge of nanocarrier. Savic et al. (2003) reported that after cellular internalization of PEG-PCL micelles by endocytosis, it localized mainly in to cytoplasm and distributed through several cytoplasmic organelles irrespective cell type.

Very few studies were carried out using varying surface density of ligand on the surface of nanocarrier (Nasongkla et al., 2004; Zhao & Yung, 2008) and its matter of interest to ascertain the effect of surface density of ligand on the extent of cellular uptake. Peptide YIGSR-NH_2 and EILDV-NH_2 was conjugated on the surface of micelles at different surface density i.e. 5 %, 10 % and 20 %. As shown in Figure 7.27 and 7.28, YIGSR at 5 % surface density increased the cell internalization of micelles (i.e. YPCL235 and YPCL570) near to two fold compared to MPCL235 and MPCL570 micelles. EPCL235 and EPCL570 at 5 % surface density showed increase in cell uptake with one and half fold compared to non conjugated micelles. With surface density of 10 % of both the peptides, YPCL235 and YPCL570 showed percent cellular uptake of 16.76 ± 2.15 and 13.30 ± 2.62 respectively while EPCL235 and EPCL570 showed 13.11 ± 2.67 and 13.28 ± 1.06 percent cellular uptakes. There was no much increase in cellular uptake observed when surface density of peptide doubled to 20 % from 10 % (Table 7.14). The result implies that after critical surface density of ligand, there was no effect of increase in ligand concentration effect on the cellular uptake enhancement. It was also reported that the high amount of intracellular folate, in the range of 2×10^7 to 9×10^7 folate molecules per cell (Leamon and Low, 1991; Lee and Low, 1994), may be responsible for the saturation and shut-off of the folate receptor uptake pathway. These findings may impede the use of nanoparticles or liposome conjugated with high amount of surface folate, however in case of peptide conjugated micelles; it is difficult to interpret the same thing in terms of concentration. The result obtained clearly supports the receptor mediated drug delivery approach using peptide conjugated PEG-PCL micelles for enhanced intracellular drug delivery.

7.4.8 Cell cycle analysis by flow cytometry

To understand how various micellar formulations affect the cell cycle progression of cancer cells, the cellular DNA content at each stage was measured with PI using flow cytometry. The study was carried out at two different subtoxic concentration of ETO and micellar formulations based on the IC_{50} values obtained. When B16F10 cells treated with free ETO and ETO loaded micelles, a reduction in fraction of cells in S phase with accumulation in G2/M phase were found as shown in Table 7.15. The cell cycle analysis carried out is showed in Figure 7.29 to 7.32.

Formulation Code	% G0-G1	% G2-M	% S	Apoptosis
UC	59.13	6.63	34.24	0.02
ETO-A	58.61	11.65	29.74	9.61
ETO-B	59.82	9.51	30.67	0.43
MPCL235-A	58.25	11.00	30.75	0.43
MPCL235-B	60.12	9.86	30.02	0.32
YPCL235-A	56.29	12.90	30.81	2.85
YPCL235-B	57.20	10.79	32.01	1.18
EPCL235-A	51.31	26.21	22.49	6.30
EPCL235-B	56.05	15.44	28.51	2.95
MPCL570-A	58.60	13.58	27.82	1.33
MPCL570-B	60.15	10.47	29.38	0.54
YPCL570-A	58.61	13.46	27.93	1.13
YPCL570-B	59.62	11.04	29.34	0.43
EPCL570-A	57.32	17.09	25.59	2.99
EPCL570-B	59.04	13.82	27.14	0.92
MPCL235-P	57.52	7.34	35.15	0.12
MPCL570-P	59.83	6.69	33.47	0.06

Table 7.15 Effect of ETO and micellar formulation induced cell cycle perturbation and apoptosis in B16F10 cells

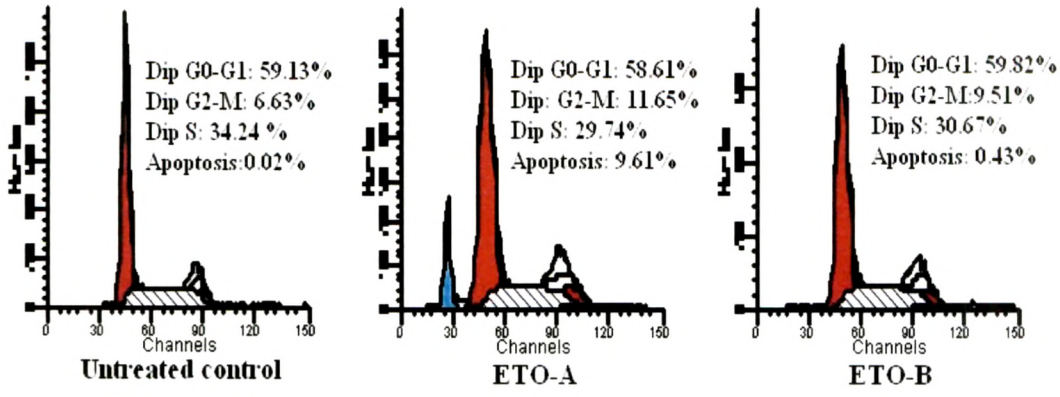

Figure 7.29 Cell cycle analysis of untreated control and ETO treated B16F10 cells

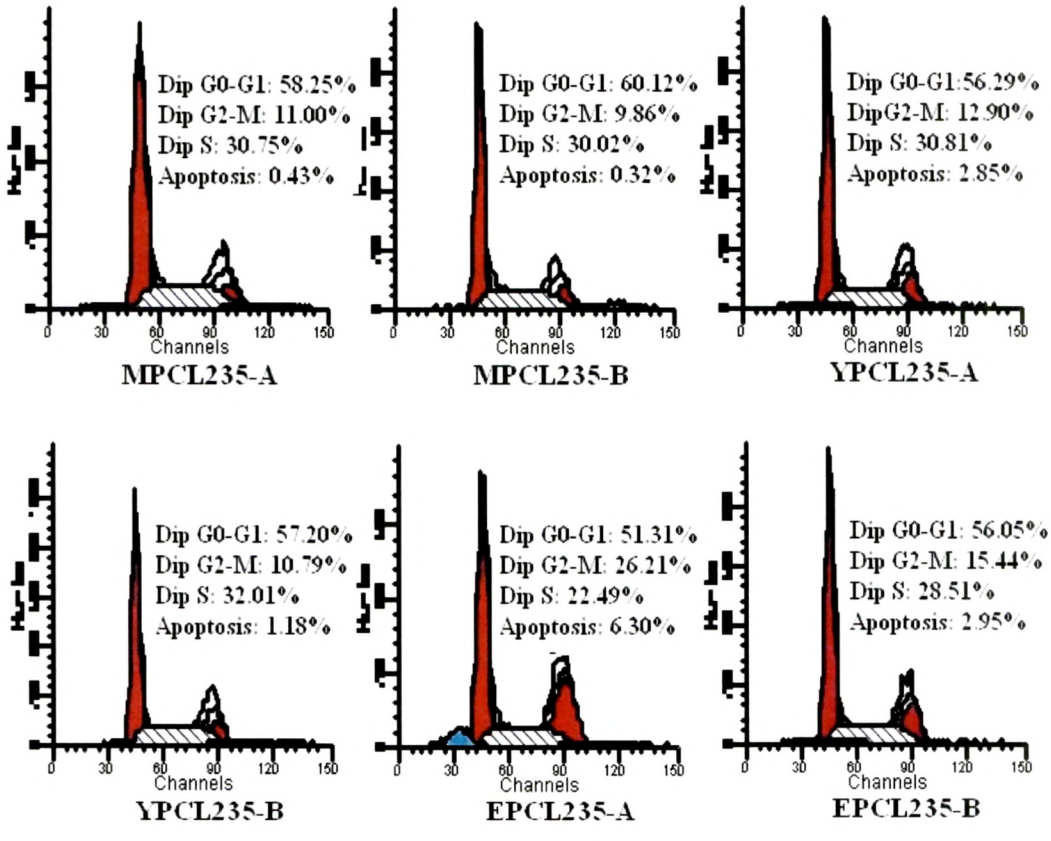

Figure 7.30 Cell cycle analysis of B16F10 cells after treatment with MPCL235, YPCL235 and EPCL235 micelles

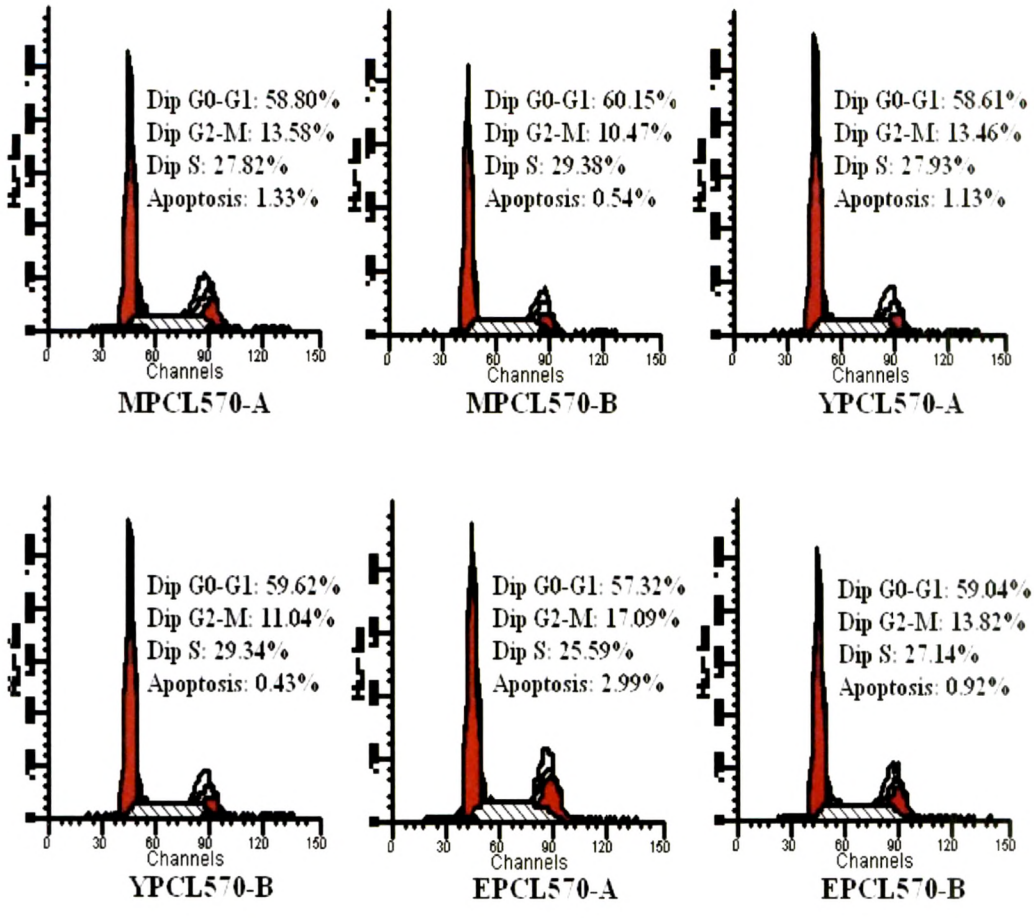

Figure 7.31 Cell cycle analysis of B16F10 cells after treatment with MPCL570, YPCL570 and EPCL570 micelles

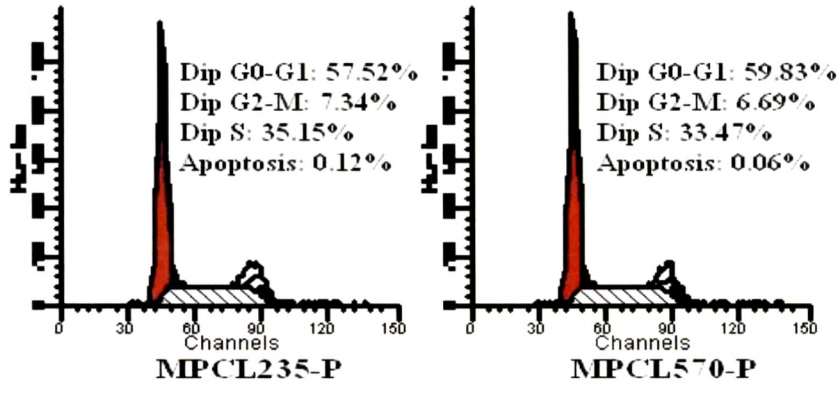

Figure 7.32 Cell cycle analysis of B16F10 cells after treatment with MPCL235-P and MPCL570-P micelles

The ETO loaded micelles showed higher percent of cell in G2-M phase compared to plain ETO. Moreover, the effect was concentration dependent, a more accumulation of B16F10 cells were observed in G2-M phase with high concentration of drug. A receptor mediated endocytosis of peptide conjugated micelles resulted in to high drug concentration in cells which has significantly increased drug induced arrest (Zhao & Yung, 2008). Moreover, ETO acts as a topoisomerase II inhibitor by forming a ternary complex. It impairs DNA synthesis progression by forming complexes with the cleaved DNA and prevents religation of the double-strand breaks in the genome of the replicating cells. Various authors reported that ETO prevents cell proliferation by G2-M phase arrest followed by apoptosis in different cancer cell line (Liu et al., 2002; Chiu et al., 2005; Nakada et al., 2006).

Apoptosis of B16F10 cells was also observed with formulations followed by G2-M phase arrest. Plain ETO with higher concentration showed 9.61 percent apoptosis. Peptide conjugated micelles showed significant apoptosis compared to non conjugated micelles. EPCL235 showed highest apoptosis of 6.30 percent. It was reported that low concentration of ETO reduces the apoptotic activity of leukaemic cell lines (Liu et al., 2002). Based on these findings, the higher percent of apoptosis observed in B16F10 cells treated by peptide conjugated micelles was due to its higher intracellular concentration of drug. Blank micellar formulation showed no any affect on cell cycle arrest as shown in Figure 7.32 and the cell cycle was similar to that of untreated control.

REFERENCES

Acharya S, Dilnawaz F, Sahoo SK. Targeted epidermal growth factor receptor nanoparticle bioconjugates for breast cancer therapy. Biomaterials 2009; 30: 5737-5750.

Alexis F, Rhee JW, Richie JP, Radovic-Moreno AF, Langer R, Farokhzada OC. New frontiers in nanotechnology for cancer treatment. Urol Oncol: Semin Ori Inves 2008; 26: 74-85.

Chiu C, Li CH, Ung MW, Fuh TS, Chen WL, Fang K. Etoposide (VP-16) elicits apoptosis following prolonged G2-M cell arrest in p53-mutated human non-small cell lung cancer cells. Cancer Lett 2005; 223: 249-258.

Davda J, Labhasetwar V. Characterization of nanoparticle uptake by endothelial cells. Int J Pharm 2002; 233: 51-59.

Desai MP, Labhasetwar V, Walter E, Levy RJ, Amidon GL. The mechanism of uptake of biodegradable microparticles in Caco-2 cells is size dependent. Pharm Res 1997; 14: 1568-1573.

Douma S, Van Laar T, Zevenhoven J, Meuwissen R, Van GE, Peeper DS. Suppression of anoikis and induction of metastasis by the neurotrophic receptor TrkB. Nature 2004; 430: 1034–1039.

Dua P, Gude RP. Antiproliferative and antiproteolytic activity of pentoxifylline in cultures of B16F10 melanoma cells. Cancer Chemother Pharmacol 2006; 58: 195-202.

Dua P, Gude RP. Pentoxifylline impedes migration in B16F10 melanoma by modulating Rho GTPase activity and actin organization. Eur J Cancer 2008; 44:1587-1595.

Dua P, Ingle A, Gude RP. Suramin augments the antitumor and antimetastatic activity of pentoxifylline in B16F10 melanoma. Int J Cancer 2007; 121: 1600-1608.

Engbring JA, Hoffman MP, Karmand AJ, Kleinman HK. The B16F10 cell receptor for a metastasis-promotingsite on laminin-1 is a heparin sulfate/chondroitin sulfate-containing proteoglycan. Cancer Res 2002; 62: 3549-3554.

Franken NA, Rodermond HM, Stap J, Haveman J, Bree CV. Clonogenic assay of cells in vitro, Nature Protocols 2006; 1: 2315-2319.

Hayot C, Debeir O, Ham PV, Damme MV, Kiss R, Decaestecker C. Characterization of the activities of actin-affecting drugs on tumor cell migration. Toxicol Appl Pharmacol 2006; 211: 30-40.

Katz D, Ito E, Lau KS, Mocanu JD, Bastianutto C, Schimmer AD, Liu FF. Increased efficiency for performing colony formation assays in 96-well plates: novel applications to combination therapies and high-throughput screening. BioTechniques for Preclinical Development 2008; 44: Pix-Pxiv.

Leamon CP, Low PS. Delivery of macromolecules into living cells: a method that exploits folate receptor endocytosis. Proc. Natl. Acad. Sci. 1991; 88: 5572-5576.

Lee RJ, Low PS. Delivery of liposomes into cultured KB cells via folate receptor-mediated endocytosis. J Biol Chem 1994; 2693198–3204.

Lefranc F, Brotchi J, Kiss R. Possible future issues in the treatment of glioblastomas: special emphasis on cell migration and the resistance of migrating glioblastoma cells to apoptosis. J Clin Oncol 2005; 23: 2411-2422.

Li X, Li R, Qian X, Ding Y, Tu Y, Guo R, Hu Y, Jiang X, Guo W, Liu B. Superior antitumor efficiency of cisplatin-loaded nanoparticles by intratumoral delivery with decreased tumor metabolism rate. Eur J Pharm Biopharm 2008; 70; 726-734.

Liang CC, Park AY, Guan JL. In vitro scratch assay: a convenient and inexpensive method for analysis of cell migration in vitro. Nature Protocols 2007; 2: 329-333.

Lillie RD. Histopathologic technic and practical histochemistry. McGraw- Hill Book Co. New York 1965; 445-446.

Liu B, Yang M, Li R, Ding Y, Qian X, Yu L, Jiang X.The antitumor effect of novel docetaxel-loaded thermosensitive micelles. Eur J Pharm Biopharm 2008; 69: 527-534.

Liu WM, Oakley PR, Joel SP. Exposure to low concentrations of etoposide reduces the apoptotic capability of leukaemic cell lines. Leukemia 2002; 16: 1705-1712.

Lopez BA, Polo D, Reig Z, Fabra A. Pentapeptide YIGSR-mediated HT-1080 fibrosarcoma cells targeting of adriamycin encapsulated in sterically stabilized liposomes. J Biomed Mater Res 2004; 69A: 155–163.

Luo L, Tam J, Maysinger D,Eisenberg A. Cellular internalization of poly(ethylene oxide)-*b*-poly(E-caprolactone) diblock copolymer micelles. Bioconjug Chem 2002; 13: 1259-1265.

Murata J, Saiki I, Azuma I. Inhibitory effect of a synthetic polypeptide, poly(Thy-Ile-Gly-Ser-Arg), on the metastatic formation of malignant tumour cells. Int J Bio Macromol 1989; 11: 97-99.

Nakada S, Katsuki Y, Imoto I, Yokoyama T, Nagasawa M, Inazawa J, Mizutani S. Early G2/M checkpoint failure as a molecular mechanism underlying etoposide-induced chromosomal aberrations. J Clin Invest 2006; 116: 80–89.

Nasongkla N, Shuai X, Ai H, Weinberg BD, Pink J, Boothman DA, Gao J. cRGD-functionalized polymer micelles for targeted doxorubicin delivery. Angew Chem Int Ed 2004; 116: 6483–6487.

Panyam J, Sahoo SK, Prabha S, Bargar T, Labhasetwar V. Fluorescence and electron microscopy probes for cellular and tissue uptake of poly(d,l-lactide-*co*-glycolide) nanoparticles. Int J Pharm 2003; 262:1-11.

Ratheesh A, Ingle A, Gude RP. Pentoxifylline modulates cell surface integrin expression and integrin mediated adhesion of B16F10 cells to extracellular matrix components. Cancer Biol Ther 2007; 6: 1743-1752.

Savic R, Luo L, Eisenberg A, Maysinger D. Micellar nanocontainers distribute to defined cytoplasmic organelles. Science 2003; 300: 615-618.

Xiaoqiang Y, Wenjing D, Liwu F, Elvin B, Jinming G, Daping Q, Xintao S. Folate-functionalized polymeric micelles for tumor targeted delivery of a potent multidrug-resistance modulator FG020326. J Biomed Mater Res 2008; 86A: 48–60.

Wojciak B, Korohoda W. Ehrlich ascites tumour cells show tissue-specific adherence and modify their shape upon contact with embryonic fibroblasts and myotubes. J Cell Sci 1990; 97: 433-438.

Woo JK, Choi DS, Tran HT, Gilbert BE, Hong WK, Lee HY. Liposomal encapsulation of deguelin: Evidence for enhanced antitumor activity in tobacco carcinogen–induced and oncogenic K-ras–induced Lung tumorigenesis. Cancer Prev Res 2009; 2: 361-369.

Yamamura K, Kibbey MC, Kleinman HK. Melanoma cells selected for adhesion to laminin peptides have different malignant properties. Cancer Res 1993; 53: 423-428.

Yoo HS, Park TG. Folate receptor targeted biodegradable polymeric doxorubicin micelles. J Control Rel 2004; 96: 273-283.

Yoshihisa K, Yoko Y, Naoki O, Yasuo T, Shinasaku N, Masa K, Mitsuko M, Koichi K, Tadanori M. Antimetastatic effect of synthetic Glu-Ile-Leu-Asp-Val peptide derivatives containing D-amino acids. Anticancer Drugs 1997; 8: 702-707.

Yuancai D, Si-Shen F. In vitro and in vivo evaluation of methoxy polyethylene glycol-polylactide (MPEG–PLA) nanoparticles for small-molecule drug chemotherapy. Biomaterials 2007; 28: 4154-4160.

Yuan H, Miao J, Du YZ, You J, Hu FQ, Zeng S. Cellular uptake of solid lipid nanoparticles and cytotoxicity of encapsulated paclitaxel in A549 cancer cells. Int J Pharm 2008; 348: 137-145.

Zastre JA, Jackson JK, Wong W, Burt HM. P-Glycoprotein efflux inhibition by amphiphilic diblock copolymers: relationship between copolymer concentration and substrate hydrophobicity. Mol Pharmaceutics 2008; 5: 643-653.

Zhao H, Yung LYL. Selectivity of folate conjugated polymer micelles against different tumor cells. Int J Pharm 2008; 349: 256-268.